Damage Reduction Strategies for a Falling Humanoid Robot

Peter Amico

Thesis submitted to the faculty of the
Virginia Polytechnic Institute and State Unviversity
in partial fulfillment of the requirements for the degree of

Master of Science

in

Mechanical Engineering

Tomonari Furukawa, Chair
Brian Y. Lattimer, Co-Chair
Alexander Leonessa
Alan T. Asbeck

August 4, 2017
Blacksburg, Virginia

Keywords: Falling, Inverted Pendulum, Impact Covers, Falling strategy

Abstract

Damage Reduction Strategies for a Falling Humanoid Robot

Peter Amico

Instability of humanoid robots is a common problem, especially given external disturbances or difficult terrain. Even with the robustness of most whole body controllers, instability is inevitable given the right conditions. When these unstable events occur they can result in costly damage to the robot potentially causing a cease of normal functionality. Therefore, it is important to study and develop methods to control a humanoid robot during a fall to reduce the chance of critical damage.

This thesis proposes joint angular velocity strategies to reduce the impact velocity resulting from a lateral, backward, or forward fall. These strategies were used on two and three link reduced order models to simulate a fall from standing height of a humanoid robot. The results of these simulations were then used on a full degree of freedom robot, Viginia Tech's humanoid robot ESCHER, to validate the efficacy of these strategies.

By using angular velocity strategies for the knee and waist joint, the reduced order models resulted in a decrease in impact velocity of the center of mass by 58%, 87%, and 74% for a lateral, backward, and forward fall respectively in comparison to a rigid fall using the same initial conditions. Best case angular velocity strategies were then developed for various initial conditions for each falling direction. Finally, these parameters were implemented on the full degree of freedom robot which showed results similar to those of the reduced order models.

General Audience Abstract

Damage Reduction Strategies for a Falling Humanoid Robot

Peter Amico

Instability of humanoid robots is a common problem, especially given external disturbances or difficult terrain. Even with the robustness of most whole body controllers, instability is inevitable given the right conditions. When these unstable events occur they can result in costly damage to the robot potentially causing a cease of normal functionality. Therefore, it is important to study and develop methods to control a humanoid robot during a fall to reduce the chance of critical damage.

This thesis proposes strategies that rotate the joints at a constant rate to reduce damage resulting from a lateral, backward, or forward fall. These strategies were used on two and three link simplistic models to simulate a fall from standing height of a humanoid robot. The results of these simulations were then used on a full robot, Viginia Tech's humanoid robot ESCHER, to validate the efficacy of these strategies.

By constant joint rotation strategies for the knee and waist joint, the simplistic models resulted in a decrease in impact velocity of the center of mass by 58%, 87%, and 74% for a lateral, backward, and forward fall respectively in comparison to a rigid fall using the same initial conditions. Best case joint rotation strategies were then developed for various initial conditions for each falling direction. Finally, these parameters were implemented on the full robot which showed results similar to those of the reduced order models.

Contents

List of Figures

List of Tables

Chapter 1

Introduction

1.1 Motivation

When we as human beings create something we design it in such a way that it is ideal for human motion or use. Therefore one can argue that a humanoid robot, capable of all human abilities and more, is the ideal form to traverse and complete tasks in a human environment. While this form comes with the advantages of being shaped as humans it also comes with its disadvantages. Most noticeably of these is the inherent instability. Since humans walk upright on two legs they have a small support polygon relative to their height and the height of their center of mass (COM). This creates a relatively small window to maintain stability while standing or walking. Therefore, creating programs to maintain stability of humanoid robots with a high number of degrees of freedom is no easy task.

In recent years there have been many advancements in whole body control for humanoid robots [1][2]. However, even with many recent advancements in humanoid motion and control, instability will always be a problem due to under-actuation (not being fixed to the ground). This instability results in falls that may cause damage to the robot resulting in a cease of normal functionality and operation. This damage can also be costly given the high cost of most robotics components. Since the goal of humanoid research is to be able to create a robot capable of handling task from the most mundane to extreme and dangerous, there must be a contingency plan in place in the event of a fall. These plans will need to include whole body control strategies designed to limit damage as the robot falls.

In 2012 the Defense Advanced Research Projects Agency (DARPA) announced

plans for the DARPA Robotics Challenge (DRC) [3]. The purpose of this competition was to investigate and test the advancements and limits of the state of the art in humanoid robots. This was driven by the recent disaster at the Fukushima nuclear reactor in Japan where a tsunami damaged equipment leading to a large scale radiation leak, the largest since Chernobyl. The intent was to have humanoid robots capable of traversing irradiated terrain near a disaster site and complete containment and repair tasks instead of exposing humans to the harsh conditions potentially causing current and future health problems. Therefore, DARPA created the DRC to mimic the potential tasks and hurtles involved in such scenarios.

In 2016 the finals for the DRC took place with 25 teams competing from around the world. While many teams were given a humanoid robot for the competition from Boston Dynamics, one of the leading humanoid robot manufacturers and researcher organizations in the world, there were several teams that manufactured and assembled their own robots. Virginia Tech was one of those teams with the creation of ESCHER [4]. ESCHER is a 32 degree of freedom humanoid robot weighing 77 kg that stands 1.78 m tall as shown in figure 1.1 [5]. During the DRC ESCHER suffered a severe fall that caused damage to both the physical components and electronics. This damage was enough to result in lack of correct operation of the robot and inability to complete any of the challenges tasks. From this experience it is clear that ESCHER requires appropriate falling damage reduction strategies to reduce the chance of this happening again.

Figure 1.1: ESCHER Humanoid Robot

1.2 Previous Works

The earliest research done on humanoid robot falling strategies was done by Fujiwara et al. who looked to the martial arts technique of breaking ones fall called UKEMI [7]. They looked at trying to impact locations on the robot with greater resistance to damage in order to reduce the chance of breakage on the robot. Following up this study the same research group focused specifically on backward falls. In this work they used an inverted pendulum with the mass at the center of mass (COM) of the robot and the pivot point at the ground contact point [8]. They allowed the length of this pendulum to change indicating a rotation of the waist and knee joint as the robot fell. During a fall, the robot was then allowed to rotate these joints as it fell in order to reduce the velocity of the COM upon impact with the ground. Further

work on backward falls done by Ma et al. showed that these rotations of the waist and knee contributed to a lowering of the COM during the fall which reduces the available potential energy of the system resulting in a lowered impact due to kinetic energy [15].

As for forward falls the strategies and models used were quite similar. Fujiwara's research group did two studies in regard to forward falls. The first used a three link inertial model to control the location of the COM to reduce angular momentum and impact force [9]. The second work furthered the first by incorporating the arms into the model and building a robot specifically designed to test falling strategies [11]. Both of these works used flexion at the knee and waist in order to reduce the velocity of the COM. Others used a similar strategy which included the arms to stop a forward fall on an object reducing impact significantly [13].

In regard to a lateral fall there are no current studies done to analyze or create falling strategies for this falling direction other than the very first paper from Fujiwara et al [7]. In this paper however, there is no description of joint strategies used or how the strategies they used were implemented. It only cites desired falling locations on the robot and the resultant impact experience from a fall on them. This leads to a look at the biomedical field. Biomechanists have studied how humans fall for a long time. Kroonenburg et al. did a study on lateral falls by human subjects who were instructed to fall to their left side onto a mat both with and without using their arms to brace [19]. This study showed that humans naturally rotated their waist and knees in order to reduce their impact with the mat.

While about half the research done in humanoid falling has been direction specific the rest have been done in the attempt to fall in a specific direction to avoid objects or land on a more protected part of the body. Yun et al. was the first to try and avoid objects when falling [20]. They considered the COM pendulum an object in 3D space and used inertial shaping to rotate the pendulum away from the object during a fall to avoid hitting it. This work was followed up by a more robust strategy by Goswami et al. who avoided several objects simultaneously with very precise inertial shaping [22]. Using the same inertial shaping but going back to the purpose of robot self protection, Lee et al. used this strategy to rotate the body during forward and lateral falls to land on the back of the robot rather than the front or side [21]. The intent of this was to land on a more structurally protected backpack rather than other more delicate parts of the body.

While the area of robot falling is small with relatively few papers there has been

significant work done in the field. Furthering this research to fill the void in lateral falling research and strategies as well as increasing knowledge for forward and backward falls will be of significant benefit to this small but important fall.

1.3 Thesis Organization

The following thesis is dedicated to the creation of joint angular velocity falling strategies to be used by the humanoid robot ESCHER in the event of a lateral, backward, or forward fall from standing height. These strategies will be analyzed using both reduced order models and full degree of freedom simulations to test their efficacy and effectiveness.

The organization is as follows. Chapter 2 will introduce the concepts needed to understand humanoid falling and develop strategies for specific falling directions using simplified models. Chapter 3 explains the need for impact dampening covers and materials and goes over why specific materials were chosen and how they were evaluated. Chapter 4 contains the simplified simulation results for the various falling strategies as well as their application to the robot in its own simulations. Finally, chapter 5 concludes the study with a summary and discussion of all results and provides insight into potential future work to be done based on the results of this work.

Chapter 2

Humanoid Falling Introduction and Background

In order to perform any task a humanoid needs a whole body controller. This whole body controller uses each movable joint to maintain stability of the robot during standing, walking, or performing tasks. While most modern controllers are capable of handling a wide range of environments and conditions, there will always be scenarios in which the whole body controller is not able to compensate for a given disturbance. In the event of unstable conditions or extreme disturbances the whole body controller will not be able to perform actions capable of returning the robot to a stable state. This can cause chaotic and unpredictable motions of the joints as the controller is still attempting to maintain stability even though its current parameters are outside the range of allowable values. To prevent against such actions and situations motion strategies must be created such that the robot is constantly in a state of programmed motion and action within its limits. In the event of a fall this means the use of preprogrammed falling strategies. These strategies must be programmed to minimize damage suffered by the robot during impact with the ground.

Given the high complexity and degrees of freedom of a humanoid robot, it is necessary to begin development of falling strategies with a simplified model. For humanoid robots, as well as for humans, the simplest accepted model used for simulation is an inverted pendulum [23]. This model uses a point mass located at the COM of the robot with a massless link extending from the COM to a pivot point on the ground. This is shown in figure 2.1.

While this model is good for many simple analyses, it only provides information

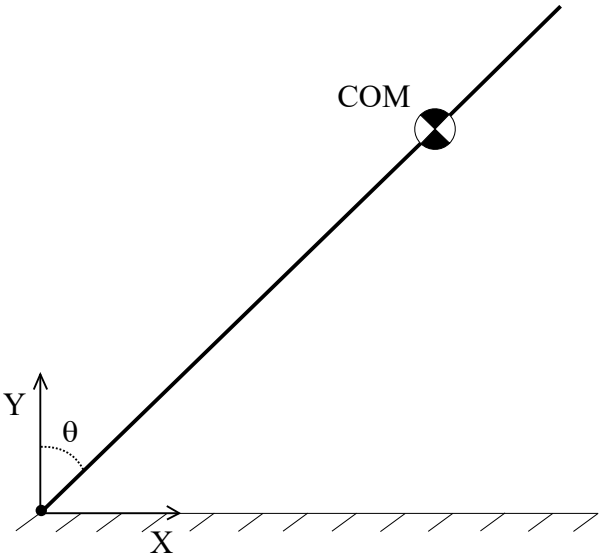

Figure 2.1: Simple Inverted Pendulum

for a body with unchanging links where all rotation takes place at the COM or ground contact point. This poses a problem as many falling strategies intend to reduce impact force by rotating various joints in order to reduce the length of the inverted pendulum.

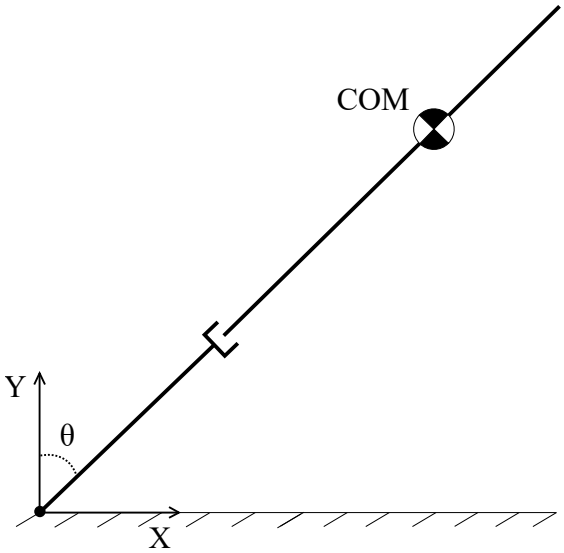

Figure 2.2: Single, variable length inverted pendulum model

To overcome this issue several researchers have made the simple adjustment of allowing the pendulum length to change during the course of the fall [8][9][12]. In figure 2.2 below, this is represented by the dashpot in the middle of the pendulum link. This dashpot represents the change in length as a controlled value rather than simply a result of applied external forces. If, however, the COM diverges from inside

the body by a significant amount this model can be inaccurate [10].

To ensure accuracy with this type of movement of the COM further alterations must be made to the model. This alteration chiefly includes the the separation of the single link into two representing the legs and torso individually as shown in figure 2.3(a). This alteration also includes the assignment of individual masses that influence the location of the COM rather than all mass located at a single point. With this separation the leg link can now be defined individually by the lengths and angle between the shank and thigh as shown in figure 2.3(b). These links do not have their own masses however as the legs are still considered only one link. With the inclusion of individual masses for the legs and torso inertial, centripetal, and Coriolis forces will now influence the motion of the COM. This will help to increase the accuracy of falling motion as these forces do play a significant role in real world motion.

Since these simulations only consider rotation in a 2D plane this model is ideal for simulating a lateral fall. While waist rotation is in the same plane as the fall knee flexion is not. This eliminates the consideration of inertial forces and rotation of the body outside the fall plane caused by knee flexion which is what is considered in a lateral fall analysis.

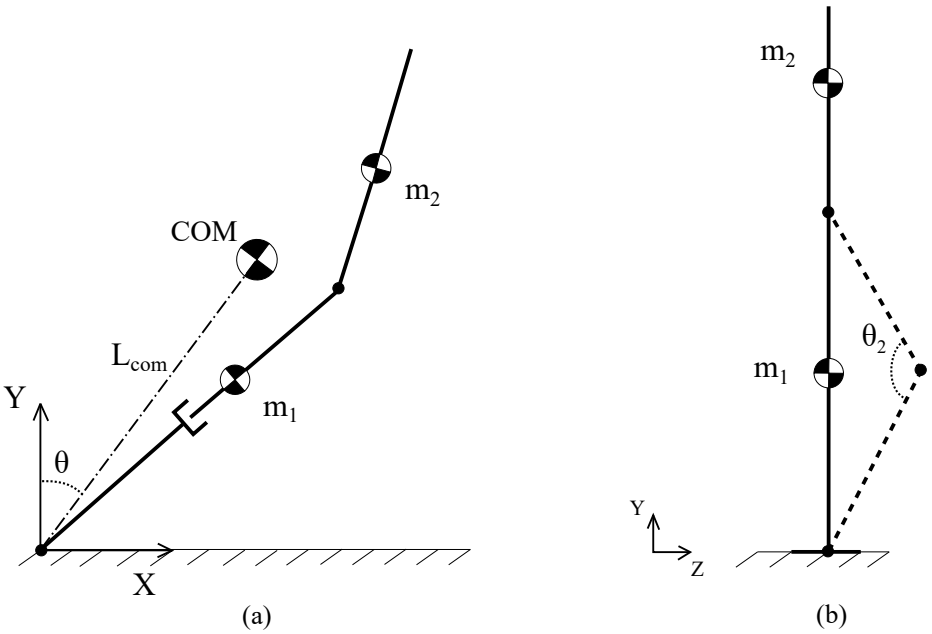

Figure 2.3: Two link fall model for lateral fall case. (a) Front view of model with variable length leg link, torso, and COM. (b) Side view of two link model with shank and thigh outside fall plane showing their interaction with leg link via knee flexion angle θ_2

For a forward and backward fall, however, both rotation of the knee and waist are done in the same plane as the fall. This allows the model to be further altered allowing the leg link to be broken up into two links representing the shank and thigh. Both the shank and thigh now have their own individual masses which will allow for incorporation of their inertial forces into the model dynamics and a more accurate calculation of the location of the COM and the resulting pendulum length. Figure 2.4(a) shows this representation for a backward fall while figure 2.4(b) represents a forward fall.

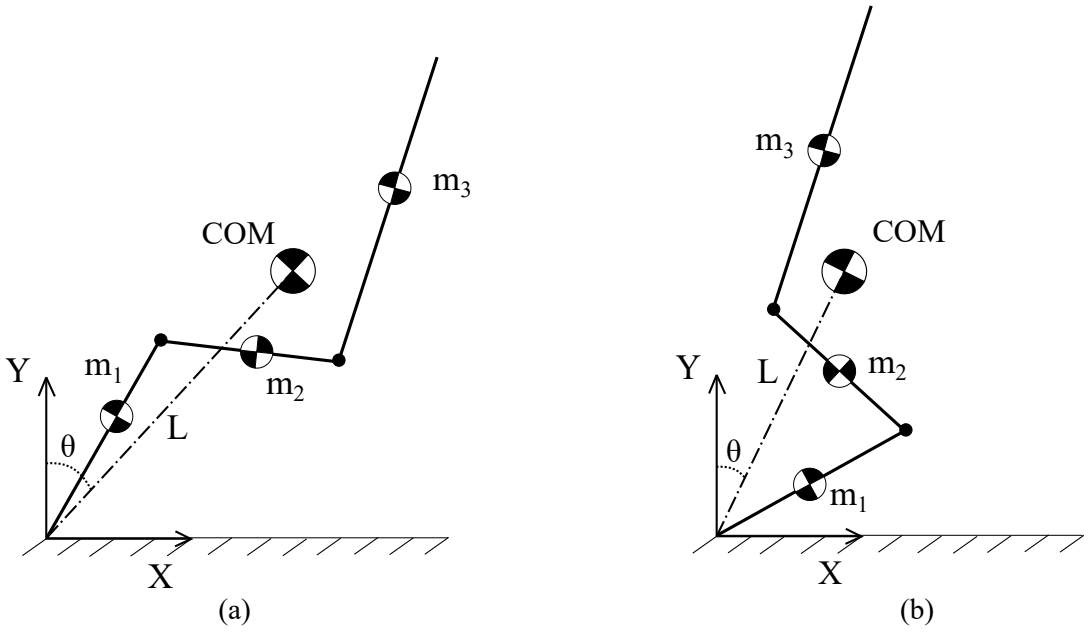

Figure 2.4: Three link fall model. (a) Backward falling model. (b) Forward falling model.

In order to use these simplified models are a representation of a full degree of freedom model, there must be some assumptions made to ensure sufficient accuracy for comparison. These assumptions are as follow.

1. All links are considered massless and completely rigid with the only mass residing at the COM of each link.

2. The point of contact with the ground (the ankle) does not leave contact with the ground at any time

3. This simulation is only valid for the fall and initial impact. No rolling or continued impacts are considered.

4. All falling is done only in a single 2D plane with no motion or rotation outside the plane considered.

As noted above the point of contact with the ground is the ankle. Given that the COM creates a large moment arm from this point it is assumed that the ankle joint is not strong enough to have an effect on the motion of a fall. This means it can be assumed any torque applied to the ankle will be insignificant. Also, it is important to note the criteria that these simulations are only valid for the initial impact with the ground. It may be the case that the location of the COM during impact with the ground will likely cause continued rotation after impact. This continued motion, however, is not considered as the results for this motion would not be valid based on the following equations used for simulation.

2.1 Impact Force Estimation

The ultimate goal of these analyses is to reduce the impact force when the robot hits the ground from a fall. For an impact of any object into another the amount of force experienced, F, is defined as the change in momentum over time. This equation (2.1) is shown below.

$$F = \frac{mv_1 - mv_2}{\Delta t} \tag{2.1}$$

In the case of impact with the unmoving ground, v_1 is the velocity just before impact, v_2 is the velocity after after impact ($v_2 = 0$), and Δt is the time taken for the robot to come to a complete stop after impact. Given that v_2 and m are constants in this equation, the only available variables to alter in the attempt to lower impact force are v_1 and Δt. It is clear from this equation that either minimizing v_1 or maximizing Δt would achieve this result..

The difficulty with maximizing Δt, however, lies in the inability to accurately estimate Δt. The amount of time taken to come to a complete stop can vary based on a number of different variables and conditions such as rebound (bouncing), breakage of parts, internal collisions, and many others which may be impossible to model accurately and even if it could be modeled it could take an impractical amount of computational power to compile. Therefore, for the sake of simplicity in modeling, we will only focus on minimizing the impact velocity of the COM during a lateral, backward, and forward fall. Maximizing Δt could be achieved, however, by the introduction of dampening materials such as protective covers.

In previous works researchers used strategies that reduced the impact velocity by employing multistage strategies that first flex and then extend the robots joints [7][12][15]. This reduces the accumulation of angular acceleration as the robot flexes and decreases the linear velocity as it extends. While the flexion strategy only requires a small enough rotational acceleration as to not exceed gravity the extension strategy requires a high enough friction value as to be able to extend the legs and waist without slipping. These strategies also require real time computation of control laws on top of the already running whole body control laws. This requires advanced computational ability in both computations per second and computations capable of being performed simultaneously. Given the short time taken for a fall to occur these strategies may not be possible to complete on-line [14]. Based on these requirements the following approaches to reduction of impact velocity employ a constant joint rotational velocity strategy that only flexes the joints inward reducing the length of the COM pendulum. This will allow for the use of a simplistic look up table capable of selecting the appropriate falling strategy for the given initial conditions. Since the strategies will only be flexing the robot joints there will also be much less concern for appropriately high friction coefficients at the ground pivot joint.

Chapter 3

Model Dynamics

Each of the following falling simulations uses one of the models from either figure 2.3 or figure 2.4. Regardless,they use the same general multi-link joint space dynamic equations. This general form equation is shown below in equation 3.1 [25].

$$\boldsymbol{M}(\boldsymbol{q})\ddot{\boldsymbol{q}} + \boldsymbol{C}(\boldsymbol{q}, \dot{\boldsymbol{q}})\dot{\boldsymbol{q}} + \boldsymbol{G}(\boldsymbol{q}) = \boldsymbol{\tau} \tag{3.1}$$

In this equation $\boldsymbol{M}$ is the inertial matrix, $\boldsymbol{C}$ is the matrix of Coriolis and centripetal forces, $\boldsymbol{G}$ is the gravitational matrix, $\boldsymbol{\tau}$ is the torque vector, and $\boldsymbol{q}$ is the generalized coordinate (in this case joint angle).

It is obvious that equation 3.1 is nonlinear as each matrix is dependent on either the joint angle or one of its derivatives. To solve this equation an iterative approach must be used as no closed form solution is capable of being obtained using current available methods. To do so the currently angular acceleration $\ddot{q}$ must first be found.

$$\ddot{\boldsymbol{q}}_{(i)} = inv(\boldsymbol{M}(\boldsymbol{q})) * (\boldsymbol{\tau} - \boldsymbol{C}(\boldsymbol{q}, \dot{\boldsymbol{q}})\dot{\boldsymbol{q}} - \boldsymbol{G}(\boldsymbol{q})) \tag{3.2}$$

Once the angular accelerations of each joint are found the angular velocities and positions can be solved for using simple integration with respect to time. Equations 3.3 and 3.4 show these results.

$$\dot{\boldsymbol{q}}_{(i)} = \dot{\boldsymbol{q}}_{(i-1)} + \ddot{\boldsymbol{q}}_{(i-1)}t \tag{3.3}$$

$$\boldsymbol{q}_{(i)} = \boldsymbol{q}_{(i-1)} + \dot{\boldsymbol{q}}_{(i-1)}t + \frac{1}{2}\ddot{\boldsymbol{q}}_{(i-1)}t^2 \tag{3.4}$$

Since the COM impact velocity will be the variable used to analyze the efficacy of each falling strategy, the location and dynamics of the COM at each iteration of the simulation must be known. The location of the COM is calculated as a function of the mass and location of the mass concentration for each individual link. While equation 3.5 represents the location for a three link model the same equation is used for a two link model by simply removing the terms multiplied by m_3.

$$COM(x_i, y_i) = \frac{m_1(x_i, y_i) + m_2(x_i, y_i) + m_3(x_i, y_i)}{m_1 + m_2 + m_3} \tag{3.5}$$

With the location of the COM known a line is drawn from the COM to the ground pivot point as shown in figure 2.3(a) and figure 2.4. This allows the calculation of the angle from the COM to vertical using the Pythagorean theorem and right triangle trigonometry.

$$L_{com} = \sqrt{COM_x^2 + COM_y^2} \tag{3.6}$$

$$\theta_{(i)} = sin^{-1}\left(\frac{COM_x}{L_{com}}\right) \tag{3.7}$$

With these found the angular velocity of the COM is then found using equation 3.8 from the difference of its current and former angle over time. In order to relate this value back to force from equation 2.1 the angular velocity must be translated into linear velocity as shown in equation 3.9. This relation will also be used to translate an initial linear velocity of the COM to initial angular velocity to simulate velocity caused by a disturbance for various cases.

$$\dot{\theta}_{(i)} = \frac{\theta_{(i)} - \theta_{(i-1)}}{\Delta t} \tag{3.8}$$

$$v = \dot{\theta} L_{com} \tag{3.9}$$

Chapter 4

Falling Strategies

4.1 Lateral Fall

In order to use a simplified 2D model of a humanoid robot all inertial rotation must take place in the same plane. For a lateral fall, this means all joint rotation must take place in the Coronal (frontal) plane. Looking at the front of the humanoid robot ESCHER, it is clear that only the waist and ankles can rotate in this plane. Therefore, the two link model, as shown in figure 2.2, must be used to accurately model the dynamics. In this case, the two legs are considered a single link which is connected to the torso at the waist. Only the inertial forces of these two links are considered in regard to body dynamics, however, flexion of the knees will indirectly affect the dynamics by shrinkage of the leg link due to knee flexion.

Figure 4.2 shows a more descriptive view of the two link robot model for this case. In figure 4.2(b) it is shown that L_1 and L_2 represent the lengths of the legs and torso respectively with L_3 and L_4 as the length of the shank and thigh. The locations and masses of each link are represented by a_1, a_2, m_1, and m_2 respectively. In figure 4.2(a), the universal coordinate q_1 defines the angle from the ground to the legs (the ankle joint) while q_2 defines the angle from the legs to the torso (the waist joint). Finally, θ_1 is the angle from vertical to the COM pendulum and θ_2 is the knee flexion angle.

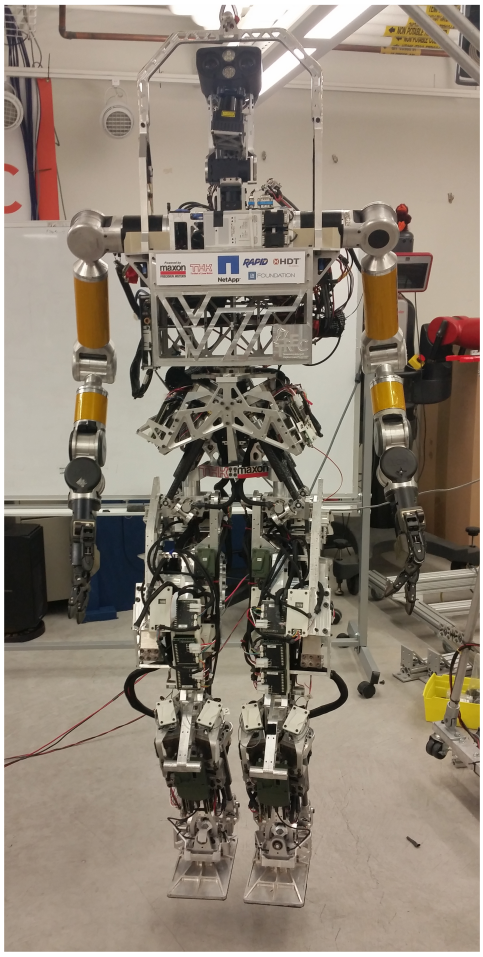

Figure 4.1: Coronal (Frontal) view of ESCHER

4.1.1 Knee Flexion Strategy

The first falling strategy used to reduce the impact velocity as first identified by Fujiwara et al. is a flexion of the knee joint [8]. This strategy reduces the COM pendulum length, L_{com}, by bringing the waist towards the ankle. When this is done directly along the COM pendulum line (when the leg link and pendulum are collinear) this strategy has the greatest impact. This is ideal as equation 3.9 shows that this reduction in L_{com} will proportionally reduce the linear impact velocity.

$$L_1 = \sqrt{L_3^2 + L_4^2 - 2L_3L_4cos(\theta_2)} \tag{4.1}$$

Using the Law of Cosines, equation 4.1 describes how the knee flexion angle and the lengths of the shank and thigh define the length of the leg link. However, since the leg length is defined with a nonlinear function and the COM is proportional to

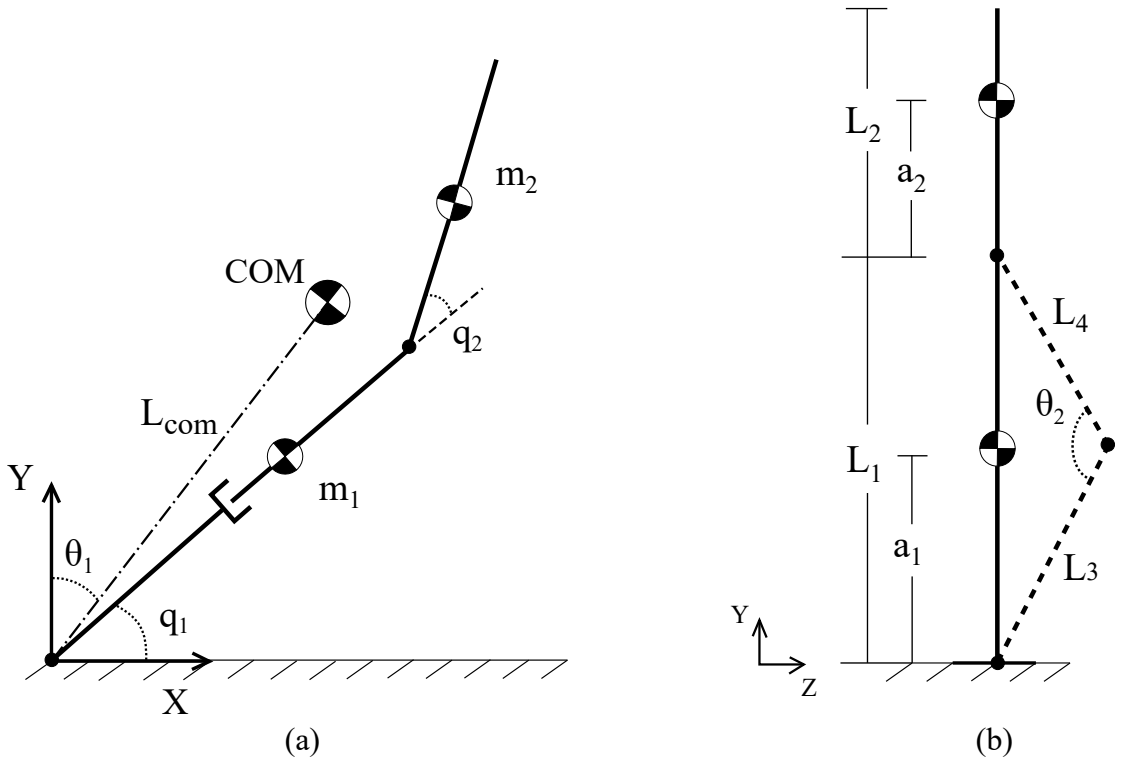

Figure 4.2: Lateral fall two link model with shank and thigh outside of fall plane resulting in the use of one variable length leg link. (a) Front view of model showing two primary links. (b) Side view of model showing shank, thigh, and knee angle impact on leg link

the mass and location of mass on each link, L_{com} is nonlinearly related to a change in flexion angle. Figure 4.3 shows how the length of this link impacts the length of L_{com}. It is clear from figure 4.3 that this relationship is nonlinear with a greater per degree impact in pendulum length reduction at smaller joint flexion angles.

4.1.2 Waist Flexion Strategy

The second strategy identified in work done by Kroonenburg et al. is rotation of the waist counter to the direction of falling [19]. In their biomechanical study they found every patient performed this strategy to dampen the impact of their fall without use of their arms. This strategy has two methods of impact reduction. The first is similar to knee flexion in that it reduces the COM pendulum length. Since the waist has a lower range of motion this impact is much less than knee flexion as shown in figure 4.3. The second is a reduced fall time by extending the waist past the COM pendulum in the direction of falling so that neither the legs nor the torso are collinear

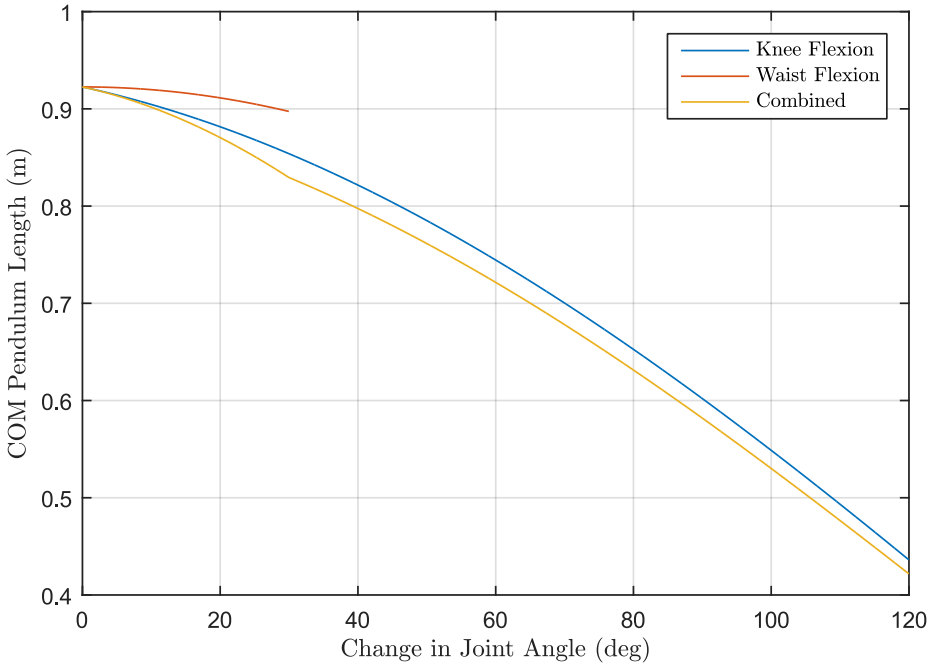

Figure 4.3: COM pendulum length as knee, waist, and combined joints are rotated from their initial angle to their limits

with the pendulum. This allows the waist to impact the ground first at a reduced impact velocity. With this strategy, however, it is likely the robot will continue to fall after first impact at the waist as the COM is further from the ground pivot point than the waist. Since, as stated in the assumptions, these simulations only analyze the initial impact it is not known how this falling strategy will effect further impacts.

Since the leg link and torso rotate in the same plane as the fall, their inertias are considered in the joint space dynamic equation (eq. 3.1). In order to maintain a constant velocity at the waist joint, proportional control with a gain of K_p is used as shown in equation 4.2. In this equation $\dot{q}_{2_{des}}$ is the desired rotational velocity of the waist joint and $\dot{q}_{2_{des}}$ is the actual velocity. To maintain a near constant angular velocity the proportional gain is set to an arbitrarily high value of 5,000. While this can create very high joint torques that may be unachievable on a real humanoid robot, the intent is to achieve idealistic results that identify how joint velocity influences impact velocity during a fall.

$$\tau = K_p \begin{bmatrix} 0 & \dot{q}_{2_{des}} - \dot{q}_{2_{act}} \end{bmatrix}^T \tag{4.2}$$

4.1.3 Combined Flexion Strategy

After analyzing strategies for rotation of the knee and waist individually, the next logical step is to analyze the use of both strategies simultaneously. This will determine if the possibility of an even greater reduction in impact velocity is possible. Based on figure 4.3 the combination of waist and knee flexion is capable of reducing the COM pendulum length more than either of the individual strategies. This reduction is not additive however, as waist flexion moves the leg link into non-collinearity with the COM pendulum. This reduces the large impact of knee flexion on pendulum length reduction. This is compensated for, however, by the reduction in fall time by early impact with the ground by the waist joint.

To perform this strategy both knee and waist flexion will be performed simultaneously at varying angular velocities. The angular velocities for both joints will then be varied in such a manner that the full range of knee angular velocities will be run for each increment of waist angular velocity. At the end of the tests the minimum impact velocity will be recorded along with the knee and waist rotational velocities that caused such a result. This, along with the results from the individual joint flexion strategies, will then be analyzed to determine the best falling strategy to reduce impact force based on impact velocity of the COM.

4.2 Backward Fall

An external disturbance in the sagittal plane will result in either a forward or backward fall. From figure 4.4 it is clear that ankle, knee, and waist rotation can occur in the same plane as a forward and backward fall. Unlike the lateral falling case, shank and thigh inertial rotation can be included in the joint space dynamic equation to more accurately simulate rotation of these joints during a fall. Figure 4.5(a) and (b) show a more detailed view of the three link model from figure 2.4(a) that will be used to simulate this case.

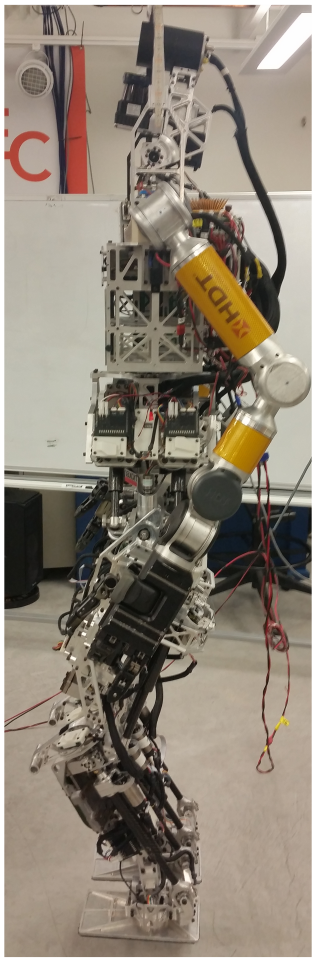

Figure 4.4: Sagittal plane view of humanoid robot ESCHER

In figure 4.5 (a) m_1 represents the mass of the shank, m_2 is the mass of the thigh, and m_3 is the mass of the torso. As in the two link model the universal coordinate q represents joint rotation with q_1, q_2, and q_3 representing the ankle, knee, and waist respectively. The COM pendulum is represented similar to the lateral fall case by L_{com} while its angle to vertical is θ. In figure 4.5(b), the lengths of each link are represented by L_1, L_2, and L_3 with the location of mass concentration of each of those links represented respectively by a_1, a_2, and a_3.

4.2.1 Knee Flexion Strategy

Since the inertial forces and individual COM locations of the shank and thigh are now included in the analysis individually, the effect of knee flexion on the COM pendulum length is slightly different. With knee flexion, the COM is no longer inside the model

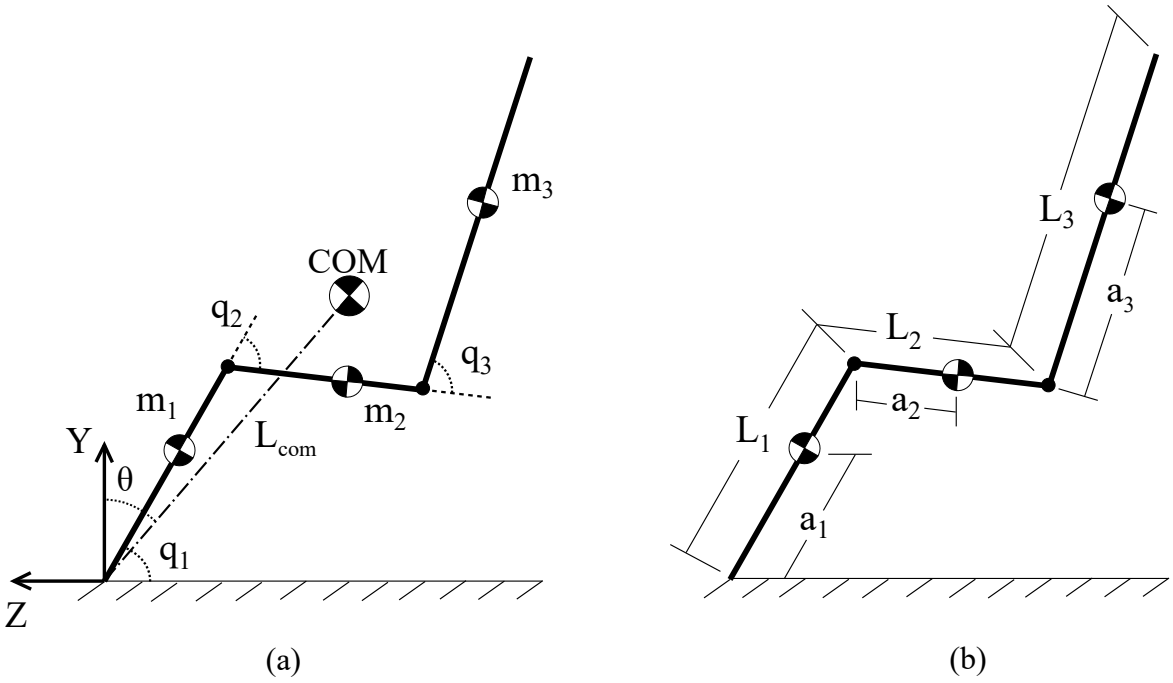

Figure 4.5: Backward Fall Three Link Model

at all times. If the waist joint remains at a constant angle with respect to the thigh the torso will rotate along with the thigh causing the COM pendulum length to both reduce and move radially. As seen in figure 4.6 this causes a greater reduction in COM pendulum length than seen in 4.3 for the two link model. Also, the inclusion of the shank and thigh inertias in the joint space dynamic equations may also have an effect on COM impact velocity. These links will create inertial, centripetal, and Coriolis forces as they rotate during the fall which may change how the system moves.

With the inclusion of the knee joint in the joint space dynamic equation, the equation for joint torques must change to incorporate it. Equation 4.3 shows the updated equation to represent this change for only knee flexion. In this case the knee joint will be rotated at a constant angular velocity while the waist will be held at its starting position. This is reflected in equation 4.3 as a desired angular velocity of the knee of $\dot{q}_{2_{des}}$ and 0 for the waist. As with the lateral falling case, this torque is derived with proportional control with an arbitrarily high gain of 5,000. This will cause almost instantaneous achievement of angular velocity and near constant angular velocity during the simulation.

$$\tau = K_p \begin{bmatrix} 0 & \dot{q}_{2_{des}} - \dot{q}_{2_{act}} & 0 - \dot{q}_{3_{act}} \end{bmatrix}^T \tag{4.3}$$

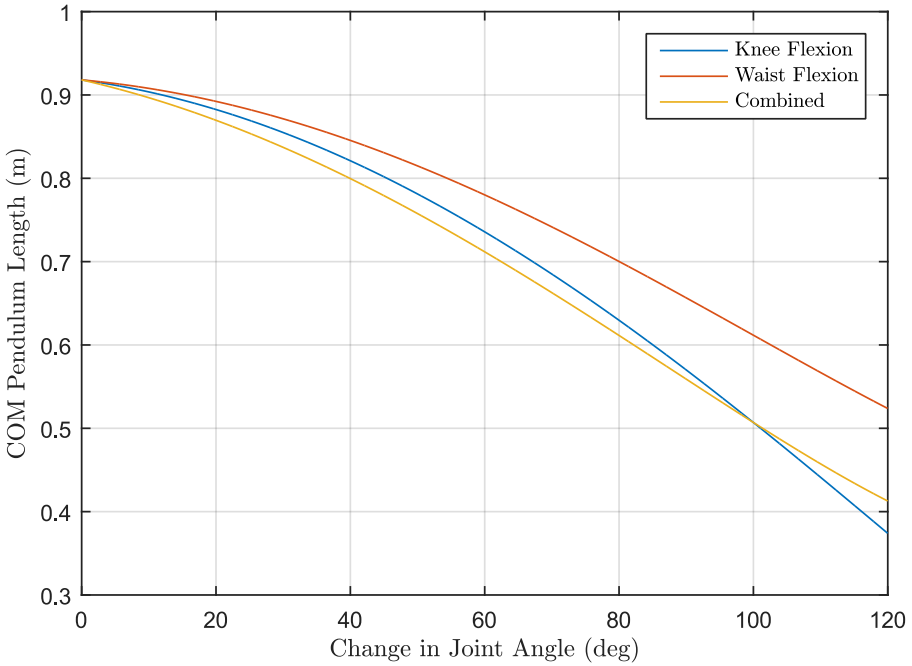

Figure 4.6: Joint rotation impact on COM pendulum length for a 3 link backward falling model

4.2.2 Waist Flexion Strategy

As compared to a lateral fall, the torso is either rotating forward towards the knees or backward towards the ground. Previous works have identified that a forward rotation of the torso towards the knees is beneficial in reduction of impact velocity by reducing both the COM pendulum length and reducing the potential energy available to the system by impacting at the waist before the COM [8][15][26]. Therefore, this is the direction of rotation that will be analyzed.

When the waist is rotated in the sagittal plane, it has a larger range of motion due to larger joint limits that enable the robot to step over objects or up stairs. Also, in most cases the range of motion in the Coronal plane of each leg individually are not symmetric with a higher range of motion in for distal rotation than proximal [5]. This limits the range of motion of the legs if they are to be used as a single entity. In the sagittal plane this is not an issue as the range of motion of the legs are symmetric allowing for use as a single entity with full range of motion. This increase in range of motion is represented in figure 4.6 where waist flexion now has a significantly higher impact on COM pendulum reduction.

To ensure the waist is the only joint performing rotation, equation 4.3 is altered in the manner shown in equation 4.4. The waist joint angular velocity $\dot{q}_{3_{des}}$ is now set to the value of choice while the knee joint rotational velocity is set to a constant 0. Similarly to the previous simulations the proportional gain is set to 5,000 to ensure near idealistic results.

$$\tau = K_p \begin{bmatrix} 0 & 0 - \dot{q}_{2_{act}} & \dot{q}_{3_{des}} - \dot{q}_{3_{act}} \end{bmatrix}^T \tag{4.4}$$

4.2.3 Combined Flexion Strategy

When both the knee and waist joint are rotated using this three link model, the COM pendulum is reduced in the manner shown in figure 4.6 as the combined case. As can be seen there is a crossover point between the combined and knee flexion strategies where knee flexion alone reduces the pendulum length more than combined rotation. This does not necessarily mean that knee flexion alone will have a greater reduction in impact velocity however. When only knee flexion occurs there is a much smaller benefit from shortened fall time due to impact with the top of the torso as compared to waist flexion where impact with the waist joint occurs much sooner. Also, impact with the top of the torso could be seen as a negative as there will be a much higher local velocity at this point than at the waist when impact at the ground occurs due to being farther from the pivot point.

To perform this strategy, angular velocity for the waist and knee joints will be achieved simultaneously by solving for both desired angular velocities as shown in equation 4.5. Similar to the lateral fall combined flexion strategy, each increment of waist angular velocity will be run with the full range of knee angular velocities in order to analyze all possible combinations of joint velocities. The linear impact velocity of the COM will be recorded from each trial and used for comparison to find the best fall strategy for the given conditions.

$$\tau = K_p \begin{bmatrix} 0 & \dot{q}_{2_{des}} - \dot{q}_{2_{act}} & \dot{q}_{3_{des}} - \dot{q}_{3_{act}} \end{bmatrix}^T \tag{4.5}$$

4.3 Forward Fall

Since a forward fall also takes place in the sagittal plane the three link model used for the backward falling case will be used for this case as well. This includes the

same incorporation of knee joint in the joint space dynamic equation which includes the shank and thigh with their individual masses and inertias. Figure 4.7 shows a detailed view of how this model is used to simulate a forward fall. All parameters for mass, angle, and length are the same as listed for the backward falling case. The only differences are the initial conditions of the model and joint rotation directions. Also, uniquely to the forward falling case in comparison to the backward and lateral fall is the ability to impact at the knee joint and lack of ability to impact at the waist joint. This ability to impact at the knees may reduce impact time due to its short length and interaction with the other two links.

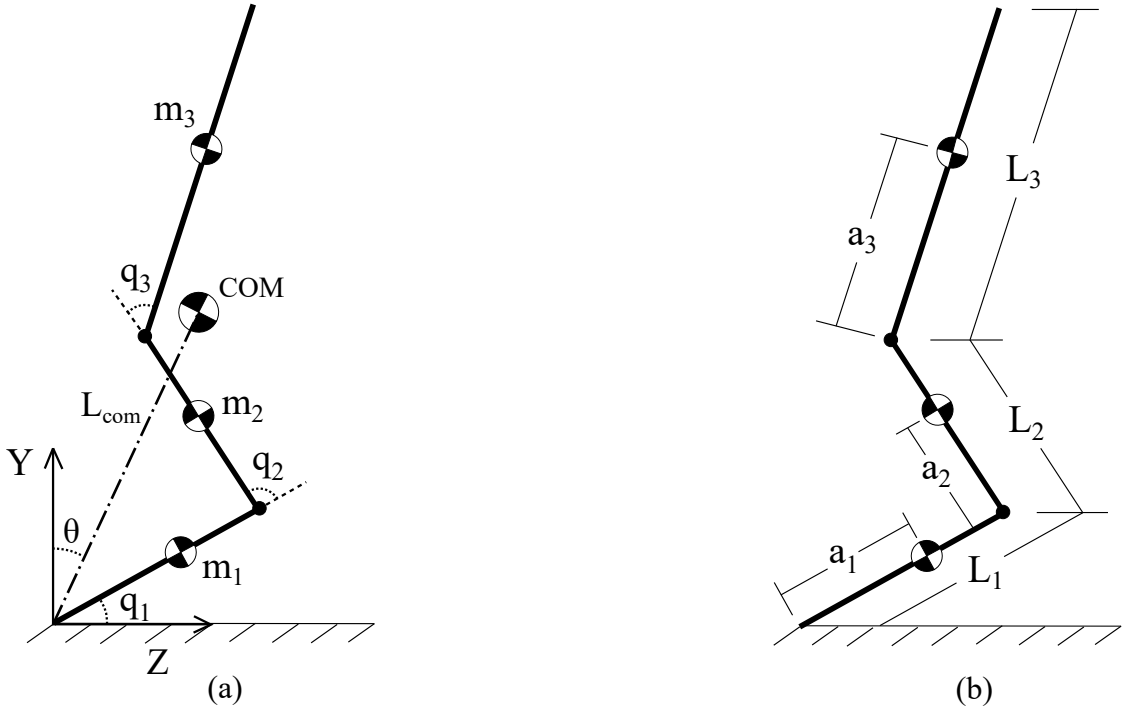

Figure 4.7: Forward Fall Three Link Model

4.3.1 Knee Flexion Strategy

In comparison to a backward fall, knee flexion during a forward fall rotates the knee joint counter to the direction of falling. Assuming no waist rotation, the thigh and torso move as a single unit towards the ankle. While this reduces the length of the COM pendulum, it has a larger impact on the rotation of the ankle joint. Since the ankle joint is already rotating the shank towards the ground, the addition of inertial forces acting in the same direction as gravity caused by the rotation of the thigh and torso act to increase the ankles angular velocity. This reduces the initial impact time

dramatically for higher angular velocities. On the contrary, this reduced impact time reduces the ability to complete full knee flexion before impact. Regardless of ability to complete the strategy, the reduction of the COM pendulum is the same as in figure 4.6 for the backward fall case. If the strategy is not capable of completion it will at least be advantageous to flex the knee joint as much as possible to take advantage of this reduction. In order to achieve angular velocities at the knee only the torque is calculated in the same manner as equation 4.3.

4.3.2 Waist Flexion Strategy

While rotation of the waist could be either forward (towards the knees and same direction of falling) or backward, this analysis will only implement rotation of the torso in the forward direction towards the knees. This decision is based on biomechanical work done by Lo et al. who found the most energy dissipation for a forward fall that included waist flexion to be with rotation of the waist towards the knees [27]. Also, if the waist were rotated in a backward direction fast enough it could cause counter rotation of the body resulting in a backward. This is not a desired result as it could cause erratic or dangerous behavior.

Forward rotation of the waist causes the torso to rotate in the same direction as falling. While this does cause additive rotation of the COM it also reduces the pendulum length. Also, if rotated fast enough and if the torso is long enough it will cause the top of the torso to impact the ground before the knee. While this may cause an increase in local velocity at the end of the torso, this analysis only considers the velocity of the COM at impact.

4.3.3 Combined Flexion Strategy

By combining the two strategies the forward rotation of the waist is countered by the backward rotation of the knees. This will decrease the COM pendulum length without the addition of increased angular velocity caused by waist rotation. In addition, rotation of the knee will have the same effect on the reduction of fall time followed by impact at the knee as it does for the individual knee flexion strategy. These conditions will reduce the impact velocity of the COM significantly.

Chapter 5

Falling Strategy Results

5.1 Introduction

The following falling strategy simulations proposed two and three link models were performed using Matlab (Mathworks®) mathematics and simulation software. To maintain consistency throughout the simulations several fixed parameters were used. These parameters were chosen to represent the ESCHER robot as closely as possible in order to compare results to full simulation results of ESCHER using the ROS Gazebo simulation software. Table 5.1 lists these constant variables for the two link model while table 5.2 list the parameters for the three link model.

As can be seen the link length L_1 and inertia value I_1 for the two link model have been omitted due to the changing length of the link. The initial value and

Table 5.1: Two link model fixed parameters

Parameter	Fixed Value
L_2	0.86 (m)
L_3	0.43 (m)
L_4	0.43 (m)
m_1	30 (kg)
m_2	45 (kg)
I_2	11.09 $(kg * m^2)$

Table 5.2: Three link model fixed parameters

Parameter	Fixed Value
L_1	0.43 (m)
L_2	0.43 (m)
L_3	0.86 (m)
m_1	15 (kg)
m_2	15 (kg)
m_3	45 (kg)
I_1	0.93 $(kg * m^2)$
I_2	0.93 $(kg * m^2)$
I_3	11.09 $(kg * m^2)$

that used for no knee flexion however, are $L_1 = 0.83$ m with an inertia value of 6.89 $kg * m^2$. Also, regardless of falling direction or trial case the torso began collinear to the pendulum line at an initial fall angle of 10° from vertical. Finally, to limit the error caused by to small of a step size for simulation, the step size for all simulations was set to 1 increment per 0.0001 second or 10,000 increments per second.

5.2 Lateral Falling Results

As stated, the lateral falling case uses the two link inertial model from figure 4.2. For this case the initial conditions were as follows: $q_1 = 80°$, $q_2 = 0°$, $\theta_1 = 10°b$, and $\theta_2 = 150°$. The knee and waist joints had limits of $\theta_2 = 30°$ and $q_2 = 30°$ which equal a range of motion of 120° and $30_\circ$ respectively. The location of the center of mass for each link was defined as half the length of each link ($a_i = 0.5L_i$) where a_1 is a able to vary based on the length of L_1. While the initial linear velocity of the COM was 0.25 m/s for the individual strategy analyses and varied for the case analyzing different initial velocities of the COM, all other initial velocities, torques, and accelerations of the model were 0 at the start of the simulation.

5.2.1 Knee Flexion Results

To analyze the linear impact velocity caused by a fall with only knee flexion, q_2 was held constant by setting $\dot{q}_{2des}$ from equation 4.2 equal to 0. Constant angular velocity of the knee was achieved by setting $\dot{\theta}_2$ to a constant value. Each subsequent simulation was run with different knee angular velocities ranging from 0 to 6 rad/s. This changed the angle of the knee at a constant rate reducing the length of L_1 by the amounts shown in figure 4.3. The velocity was assumed to be instantaneously achieved and thus started at increment 1. The knee joint was rotated at all times during the simulation unless the joint limit of $\theta_2 = 30°$ was reached. At this point θ_2 was set to 0 and the knee flexion angle was held at this value until the model impacted the ground.

As a baseline for comparison, a rigid fall (no waist or knee rotation) was performed resulting in an impact velocity of 3.49 m/s. Figure 5.1 shows the results of performing knee flexion at varied angular velocities. The minimum impact velocity of 1.88 m/s was experienced at a knee angular velocity of 2.33 rad/s which is a reduction of 46% from the rigid fall case.

These results show a behavior as to be expected. Based on equation 3.9 it is known that a longer COM pendulum length will result in higher impact velocities. Therefore, decreasing this length will reduce the impact velocity proportionally. Since knee flexion has a nonlinear relationship with pendulum length this results in nonlinear decreasing exponential behavior from a linear increase in knee angular velocity until the minimum is reached. This point is the minimum knee angular velocity required to complete full flexion of the knee. After this point the impact velocity gets larger which is also expected. If the knee joint has completed full flexion before impact with the ground there will still be rotation of the now rigid model. This continued rotation will have a positive acceleration due to gravity causing an increase in impact velocity. Also, since the inertias of the shank and thigh are not considered in the dynamic equations there is no influence of their inertial, Coriolis, or centripetal forces on the fall which causes the smooth results.

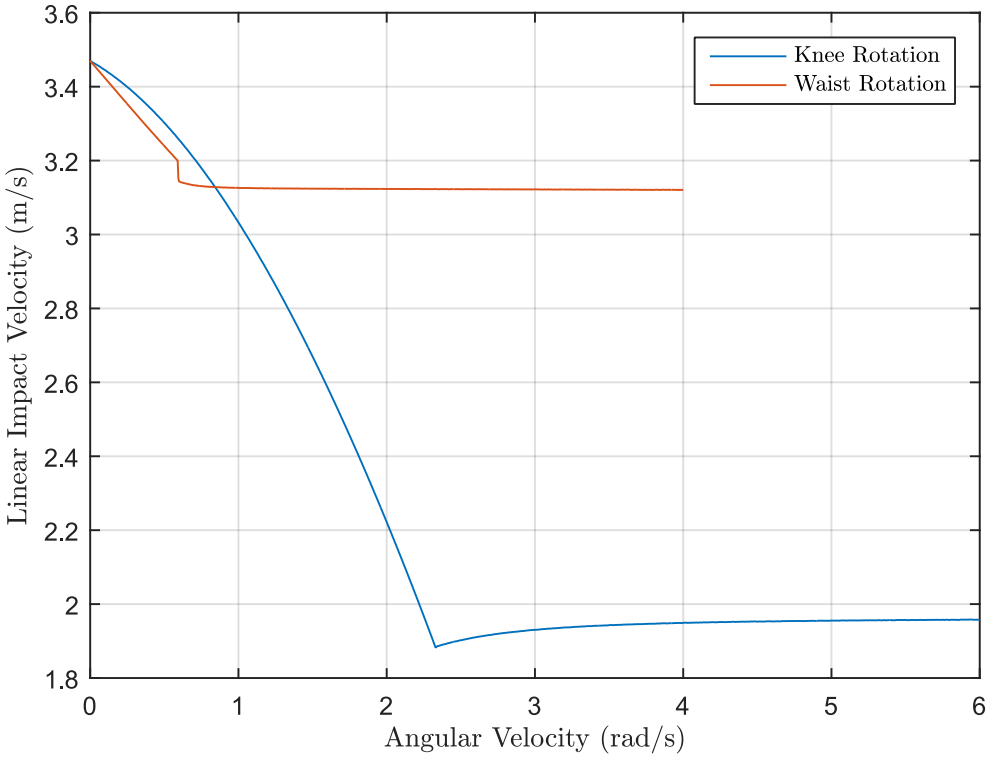

Figure 5.1: Lateral Fall Impact Velocity vs Joint Rotational Velocity

5.2.2 Waist Flexion Results

The second analysis was done for only waist flexion in a direction counter to that of falling. The knee flexion angle was held constant at $\theta_2 = 150°$ resulting in a constant length $L_1 = 0.83$ m. To hold the waist rotational velocity constant $\dot{q}_{2des}$ from equation 4.2 was set to the desired velocity. Since the gain was set to a high value the and began at increment 1 the achievement of rotational velocity was almost instantaneous. As with the knee flexion strategy, waist rotation was allowed to take place until the joint limit was reached at which point $\dot{q}_{2des}$ was set to 0 and held until the simulation ended.

The waist rotational velocity was varied from 0 to 4 rad/s resulting in the impact velocities shown in figure 5.1. For this case the minimum impact velocity was 3.12 m/s at a angular velocity of 4 rad/s resulting in a 11% reduction. Unlike the knee flexion strategy this was not the minimum required rotational velocity for waist flexion to complete before impact. This velocity can be noted by the step down response at 0.6 rad/s. It is important to note however that after this point the impact velocity appears to approach 3.12 rad/s asymptotically.

The difference in these results compared to the knee flexion case are expected. Since the waist rotates the torso link who's inertia is considered in the joint dynamic equation the result is expected to not be a smooth response. The step down result at 0.6 rad/s is due to the motion of the COM no longer including rotation of the waist. This sudden stop in rotation causes the velocity of the COM to slow down and only move due to the effect of gravity. While this is similar to the initial rigid case of no joint rotation it is decreased due to the smaller COM pendulum length and lessened fall time due to early impact at the waist.

5.2.3 Combined Flexion Strategy Results

The third analysis done for a lateral fall involves combining the knee and waist rotation strategies. This strategy uses the same initial conditions and joint limits as the previous two but allows for rotation of both joints simultaneously. Each trial was done using one constant velocity for the waist and one for the knee. Figure 5.3 shows the results of these trials. The minimum impact velocity of 1.47 m/s was experienced using a knee angular velocity of 0.38 rad/s and a waist angular velocity of 1.52 rad/s resulting in a 58% reduction in impact velocity from the rigid fall case. Similar to the

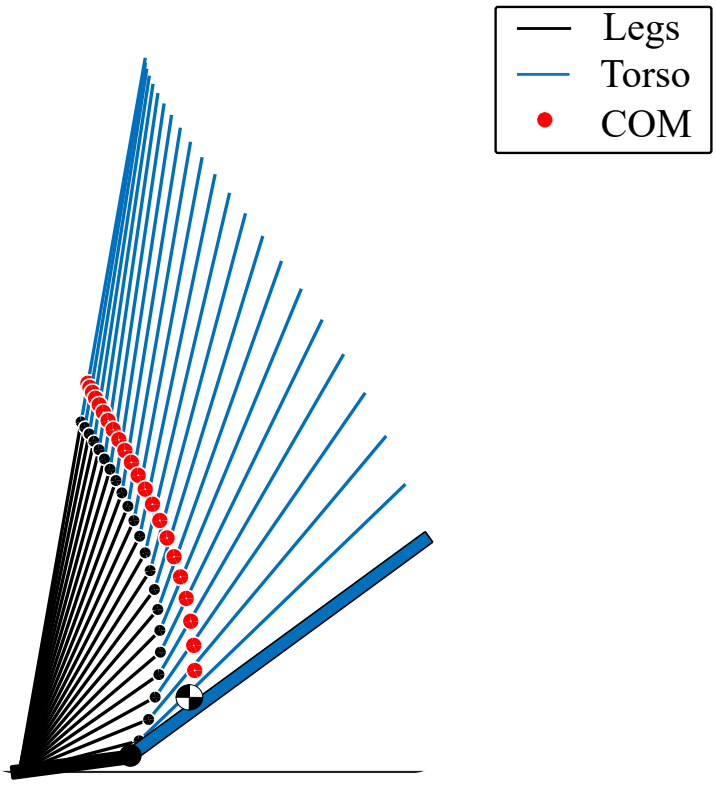

Figure 5.2: Best case lateral fall simulation for an initial velocity of 0.25 m/s

knee flexion strategy, both of these angular velocities were the minimum necessary to complete both rotational strategies before impact with the ground.

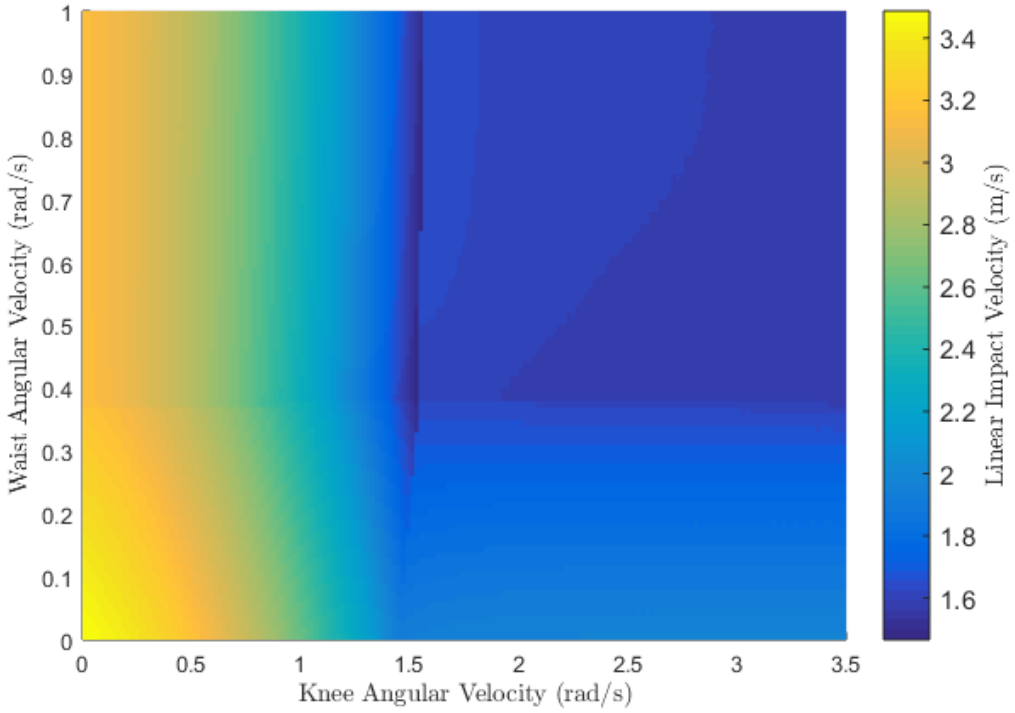

Figure 5.3: Lateral Fall Impact Velocity vs Combined Rotational Velocities

5.2.4 Combined Flexion Strategy Results for Various Initial Velocities

In order to account for various potential initial linear velocities a final group of simulations were run. The initial linear velocity was varied from 0 to 1.0 m/s in increments of 0.1. Each increment had the same joint limits as the previously run simulations and were run in the same manner. These results are shown in table 5.3. These results shows a clear increase in both knee and waist angular velocity in order to achieve the minimum impact velocity for an increasing initial linear velocity. Interestingly the minimum impact velocity of the COM gradually decreases as the initial velocity increases. This may be due to the shorter fall time at with higher initial velocities.

Table 5.3: Best Case Lateral Combined Falling Strategy Results with Varying Initial Linear Velocity

Initial Vel (m/s)	Knee Vel (rad/s)	Waist Vel (rad/s)	Impact Vel (m/s)
0.0	0.0	0.0	3.49*
0.0	2.15	0.55	1.35
0.1	2.30	0.60	1.35
0.2	2.40	0.65	1.35
0.3	2.55	0.65	1.30
0.4	2.65	0.70	1.32
0.5	2.80	0.70	1.28
0.6	2.90	0.75	1.29
0.7	3.05	0.80	1.26
0.8	3.20	0.80	1.21
0.9	3.30	0.85	1.23
1.0	3.40	0.90	1.25

*Impact velocity for rigid fall shown for reference

5.2.5 Full Degree of Freedom Robot Simulation

To test the efficacy of these strategies and the simplified model, the ROS Gazebo simulation package was used to simulate falling of the Virginia Tech ESCHER robot [24]. Each of the various strategies was tested along with a rigid fall case to as a comparison. Figure 5.4 shows the results from these tests using acceleration data read from the internal measurement unit with simulated noise on the robot as an indication of impact force. This data is the combined magnitude from the X, Y, and Z axis' to eliminate the need to compare forces experienced in different directions.

Unfortunately, since a lateral fall causes movement of many components that impact at different times and in different ways the results are quite noisy. It is clear, however, that a rigid fall has the highest impact single impact with an impact acceleration of 612 m/s^2. Waist flexion shows a significant decrease over the rigid falling case with an impact acceleration of 279 $m//s^2$ followed by knee flexion at 217 m/s^2 and finally the combined flexion case at 144 m/s^2. This shows a reduction of 54%, 65%, and 76% for the waist, knee, and combined strategies respectively over the

rigid falling case.

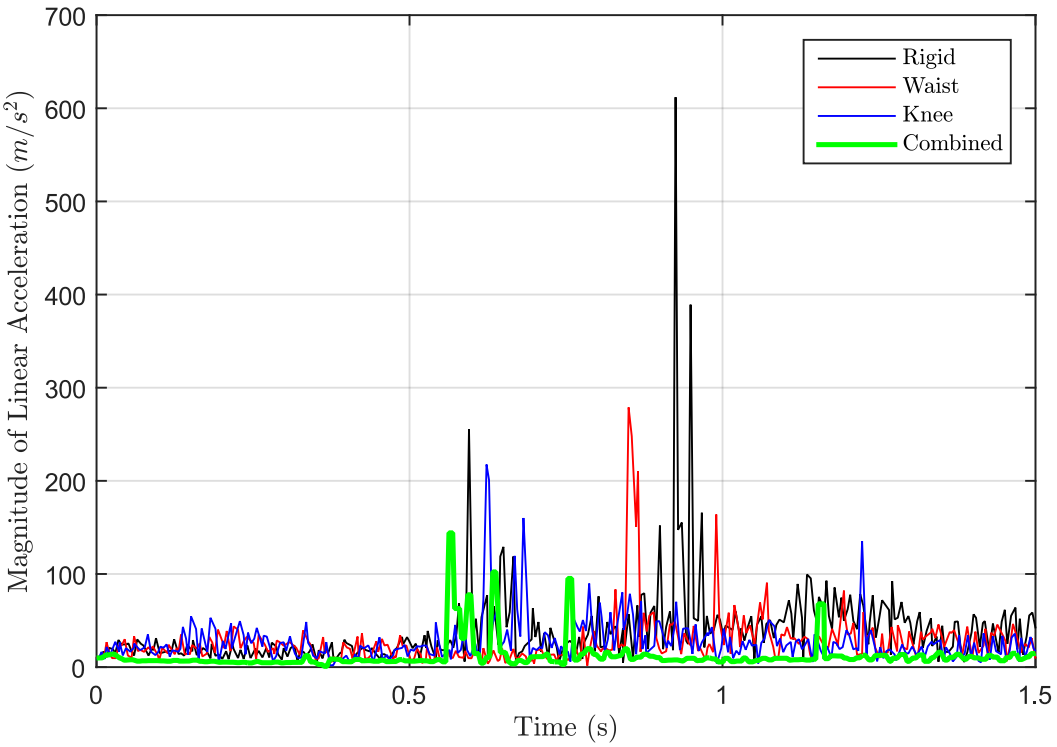

Figure 5.4: Simulation data from ESCHER robot using ROS Gazebo simulation

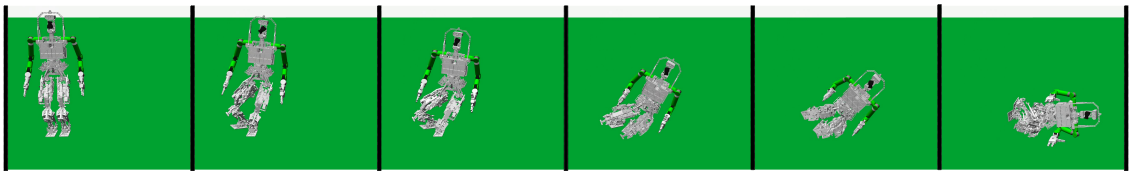

Figure 5.5: ESCHER full degree of freedom lateral fall simulation in ROS Gazebo

5.3 Backward Falling Results

To set up the simulations for a backward fall using the model shown in figure 4.5. The initial conditions for the simulations were $q_1 = 95°$, $q_2 = -30°$, $q_3 = 15°$, with limits of $q_2 = -150°$ and $q_3 = 150°$. Similar to the two link model, the location of the center of mass for each link is located at half the total length of the link ($a_i = 0.5 * L_i$). Excluding the initial velocity of the COM which was 0.25 m/s in the negative Z axis for all cases, the initial velocities, accelerations, and torques of all joints were set to 0.

5.3.1 Knee Flexion Results

For only knee flexion during a backward fall, the desired angular velocity for the waist joint q_{3des} was set to 0 as shown in equation 4.3. To rotate the knee at a constant angular velocity q_{3des} was set to a single value ranging from 0 to 8 rad/s. As with the lateral simulations the knee joint was rotated until it hit the joint limit of $q_2 = -150°$ at which point q_{2des} was set to 0 to stop rotation and the model was allowed to continue falling until impact with the ground.

Results of these simulations is shown in figure 5.6. The reference case of 0 rad/s is shown to result in a COM linear impact velocity of 3.49 m/s. While there is no local minimum unlike the lateral case, the minimum for this range of angular velocities was 1.05 m/s at 8 rad/s which is a 70% reduction. Similar to the waist strategy for the lateral case there is a step down in the linear impact velocity at 2.75 rad/s. This angular velocity is the minimum required to complete knee flexion before impact.

It is important to note that since the waist does not move relative to the thigh each simulation ends with impact at the top of the torso instead of the waist. This has a similar effect as rotation of the waist in that the top of the torso impacts before the COM which reduces the fall time. This may not be desirable in all cases as this part of a robot may not be as structurally strong as the waist or back of the torso. The reduction of impact velocity by this strategy however is at least significant enough to drastically reduce damage.

5.3.2 Waist Flexion Results

For the waist flexion strategy, counter to the knee flexion strategy, q_{3des} was set to a single constant velocity while q_{2des} was set to 0 to ensure only rotation at the waist joint. The angular velocity of the waist was varied from 0 to 8 rad/s in order to observe the full range of behaviors of linear impact velocities. These results are shown in figure 5.6. From this figure there is clearly a local minimum at an angular velocity of 3.0 rad/s and a local maximum at 5 rad/s. The total minimum impact velocity of 1.76 m/s was, similar to knee flexion, experience at a waist angular velocity of 8 rad/s. This resulted in a 50% reduction in impact velocity.

The local minimum and maximum show interesting behavior caused by the influence of inertial forces. The local minimum of 3.0 rad/s results in the torso ending perpendicular to the COM pendulum at the time of impact. After this point the im-

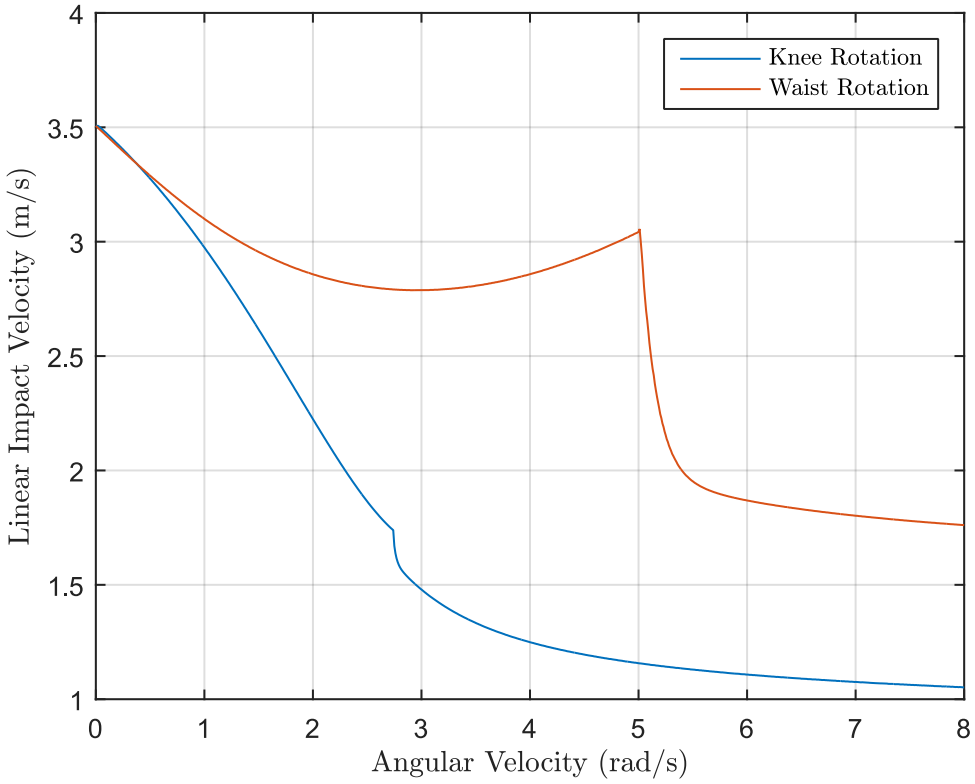

Figure 5.6: Backward Fall COM Impact Velocity vs Joint Angular Velocity

pact velocity increases due to the rotation of the waist contributing to an increase in angular velocity of the COM during falling. The local maximum represents minimum velocity required to complete the waist flexion strategy. This is why there is such a sharp decline in impact velocity at this point. Once full flexion has occurred the system rotates as a rigid body as a result of only gravity until impact. If the joint limit of the waist was smaller or the range of motion reduced this peak would either not exist or would be much smaller.

5.3.3 Combined Flexion Results

The results for the combined joint rotation strategy are shown in figure 5.8. This analysis was done using the same range of joint angular velocities as the individual analyses. These simulations were run in the same manner as the lateral falling case with each simulation using only one angular velocity for the knee joint and one angular velocity for the waist joint during any individual simulation. To compare, the full range of angular velocities for the knee joint were run for every increment of waist

angular velocity. As a baseline for comparison the rigid falling impact velocity was 3.49 m/s

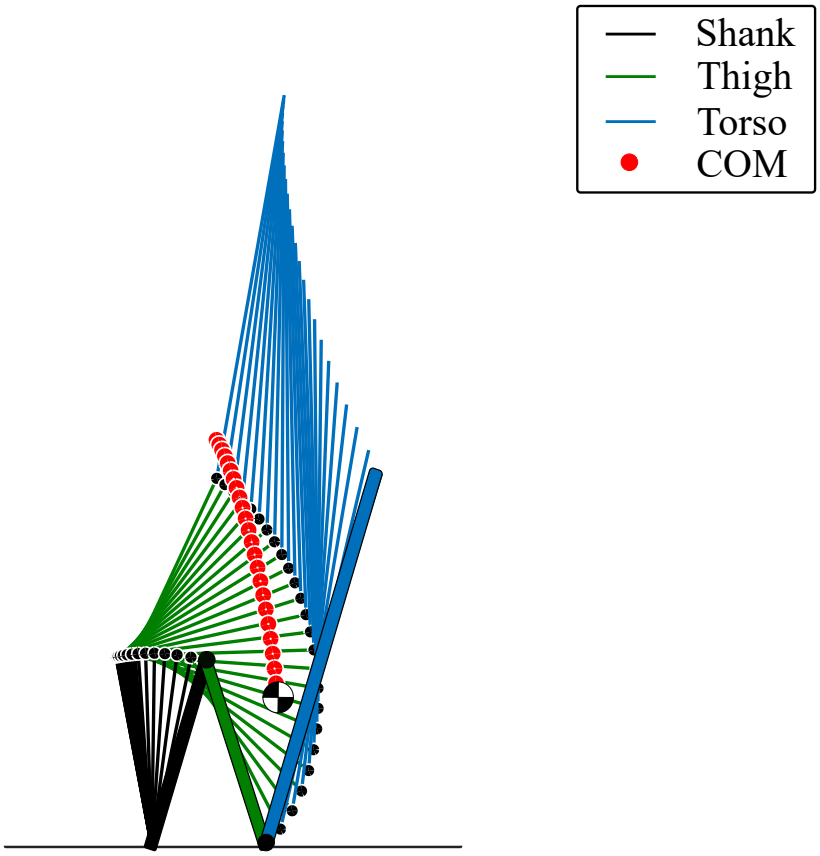

Figure 5.7: Best case backward fall simulation for an initial velocity of 0.25 m/s

The minimum impact velocity of 0.44 m/s was experienced with a knee angular velocity of 5.2 rad/s and a waist angular velocity of 8 rad/s resulting in an 87% reduction in impact velocity. This particular set of parameters was the highest possible angular velocity for the waist and the minimum angular velocity required to complete knee flexion in the given fall time. This result is interesting as it would be expected from the individual results that the highest possible knee flexion value would result in the lowest impact velocity. There is also a noticeable drop in impact velocity at the minimum angular velocity required to complete waist flexion. This point where both rotations complete just before impact results in 0.50 m/s impact velocity. This indicates that any increase in angular velocity of the waist or knee may be not worth the effort due to a decrease of only 2% in impact velocity at best from the lowest impact velocity. Also, in a real world scenario higher velocities may be unachievable due to hardware limits.

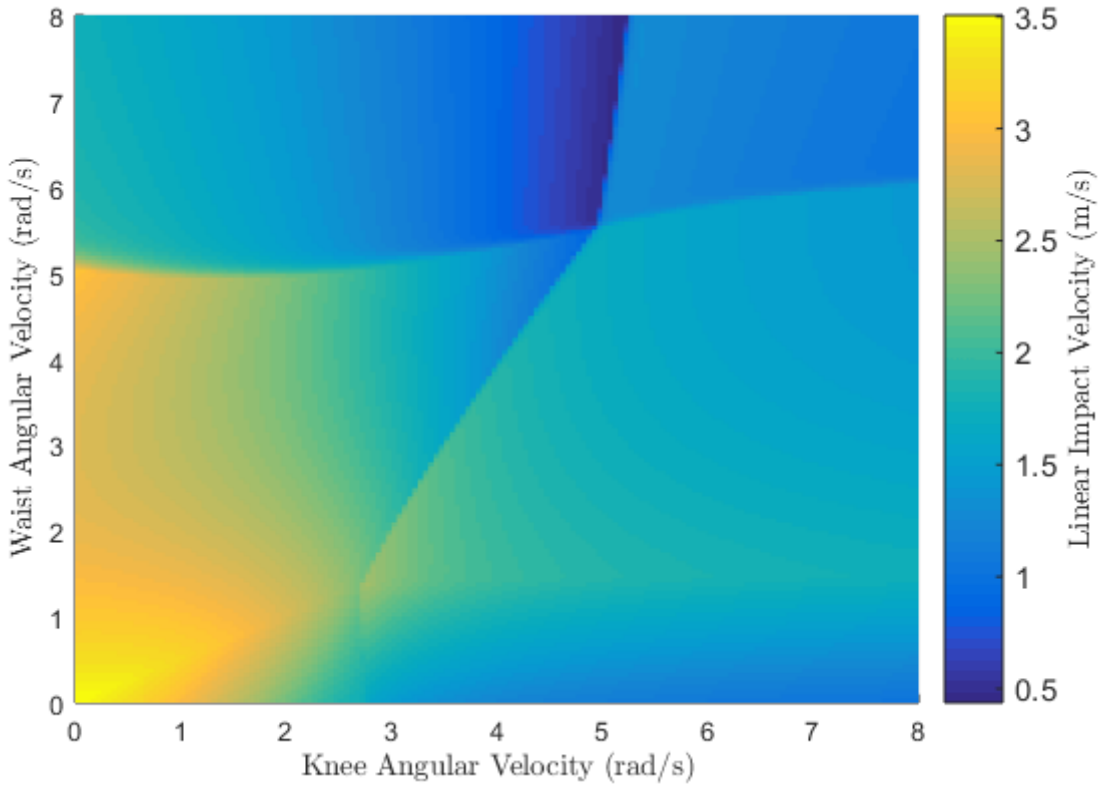

Figure 5.8: Backward Fall Impact Velocity vs Simultaneous Joint Angular Velocity

5.3.4 Combined Strategies for Various Initial Velocities

Given that a fall is likely to come from a variety of different conditions, a final test was done to analyze the effect of various initial velocities of the COM. These simulations used the combined flexion strategy as it showed the best reduction in impact velocity. The minimum impact velocities as well as the best case parameters used to achieve them are shown in figure 5.4. There is a clear pattern of maximum waist angular velocity with increasing knee velocity. This appears to follow the trend seen in the individual analysis for the combined flexion strategy. Also, it should be noted that there is a jump in minimum impact velocity at an initial velocity of 0.8 m/s. At this initial velocity the waist cannot complete full flexion before impact with the ground even at the maximum speed thus resulting in higher impact velocity.

Table 5.4: Best Case Backward Combined Falling Strategy Results with Varying Initial Linear Velocity

Initial Vel (m/s)	Knee Vel (rad/s)	Waist Vel (rad/s)	Impact Vel (m/s)
0.0	0.0	0.0	3.49*
0.0	4.00	7.80	0.51
0.1	4.40	7.90	0.48
0.2	4.80	7.85	0.46
0.3	5.20	7.70	0.44
0.4	5.65	7.90	0.42
0.5	6.10	7.90	0.41
0.6	6.55	7.85	0.40
0.7	7.00	8.00	0.45
0.8	7.25	8.00	1.05
0.9	7.40	8.00	1.12
1.0	7.50	7.95	1.13

*Impact velocity for rigid fall shown for reference

5.3.5 Full Degree of Freedom Robot Simulation

As with the lateral falling case the efficacy of these strategies was tested on the full degree of freedom, Virginia Tech ESCHER robot in simulation in Gazebo. The results from these tests are shown in figure 5.10. As expected, the rigid falling case has the highest impact acceleration at 1000 m/s^2 followed by waist flexion at 835 m/s^2, knee flexion at 620 m/s^2, and combined flexion at 237 m/s^2. This resulted in a reduction of 17%, 67%, and 76% for the waist, knee, and combined flexion strategies over the rigid falling case.

The multiple peaks seen for both the waist and combined flexion case show further impacts after the initial impact with the ground caused by rolling. Since these analyses did not consider the effects of these strategies after initial impact, this rolling behavior is not considered in regard to efficacy of each strategy. They are important to note, however, which is why they were included in this figure. Also, it is important to note that even with rolling after the initial impact, the impact force of the continued impacts for the combined case were smaller than any of the highest impacts for the other three cases.

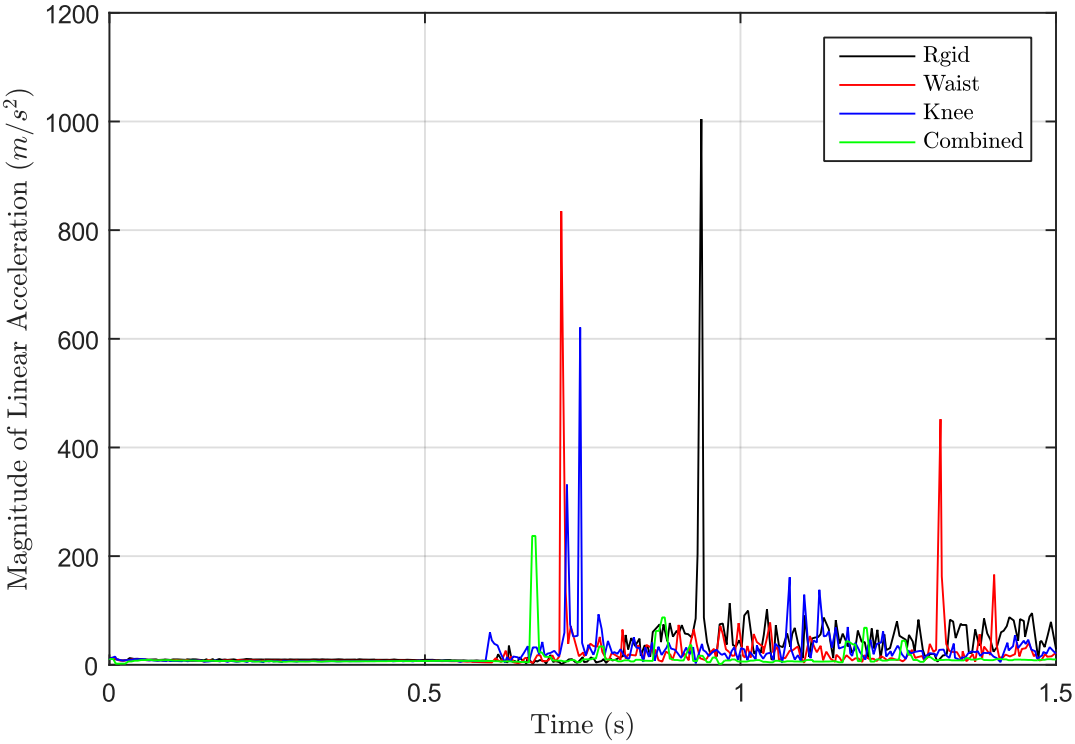

Figure 5.9: ESCHER full degree of freedom backward fall simulation results in ROS Gazebo

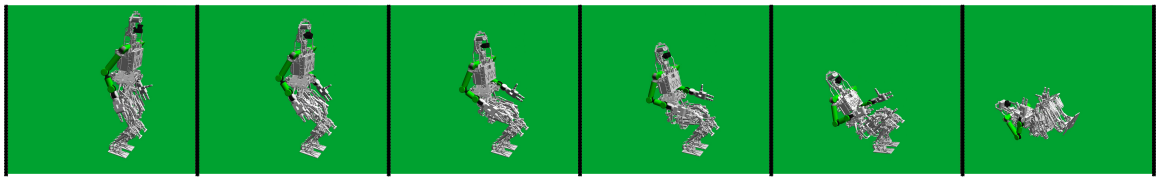

Figure 5.10: Escher full degree of freedom backward fall simulation in ROS Gazebo

5.4 Forward Falling Results

Using the model from figure 4.7, the forward falling simulation parameters were identical to the backward falling case with a few exceptions. The initial linear velocity of the COM, 0.25 m/s cause a rotation of the body towards the positive Z axis initiating a forward fall. Also, the initial joint angles of the model were $q_1 = 73°$, $q_2 = 30°$, and $q_3 = -15°$.

5.4.1 Knee Flexion Results

As with the backward falling case, the desired angular velocity of the waist joint was set to 0 as shown in equation 4.3 to analyze only knee flexion. Knee flexion was analyzed by varying the angular velocity of the knee joint from 0 to 8 rad/s. Once the model impacted the ground ending the simulation the COM impact velocity was calculated.

The results of these knee flexion simulations are shown in figure 5.11. The minimum impact velocity of the COM was 1.17 m/s at a knee angular velocity of 7 rad/s resulting in a reduction of impact velocity compared to the rigid fall case with an impact velocity of 3.1 m/s, of 62% . While the results look similar to the backward fall case, there is the noticeable omission of the step down response and the reduced impact velocity of the rigid fall case. The later of these differences is due to early impact at the knee before the COM reaches the ground in all cases. The former is due to the lack of ability to complete full knee flexion before impact with the ground. Since knee flexion causes the thigh and torso to rotate toward the ankle it increases the speed at which the ankle rotates the knee toward the ground shortening the time until impact. Lastly, there is a slight increase in impact velocity after the minimum at 7 m/s which would indicate that rotation of the knee causes movement of the COM in the same direction of falling increasing its velocity.

5.4.2 Waist Flexion Results

Waist flexion was performed exactly the same as in the backward falling case with waist rotation causing the torso rotate towards the knees. This strategy was also simulated with velocities ranging from 0 to 8 rad/s. The results of these simulations are also shown in figure 5.11 with a minimum impact velocity of 1.32 m/s at 8 rad/s. This resulted in a 57% reduction from the rigid falling case.

The first section of interest in these results is the maximum at 0.7 rad/s. Before this point the torso rotates toward the knees causing an increase in angular velocity of the COM with very little decrease of the COM pendulum length resulting in the increase in impact velocity. After this point the torso rotates fast enough for the end of the torso to impact the ground before the knees resulting in a much shorter fall time. This is the case with all angular velocities higher than this value.

The second section of interest is the local minimum and local maximum at 3.32

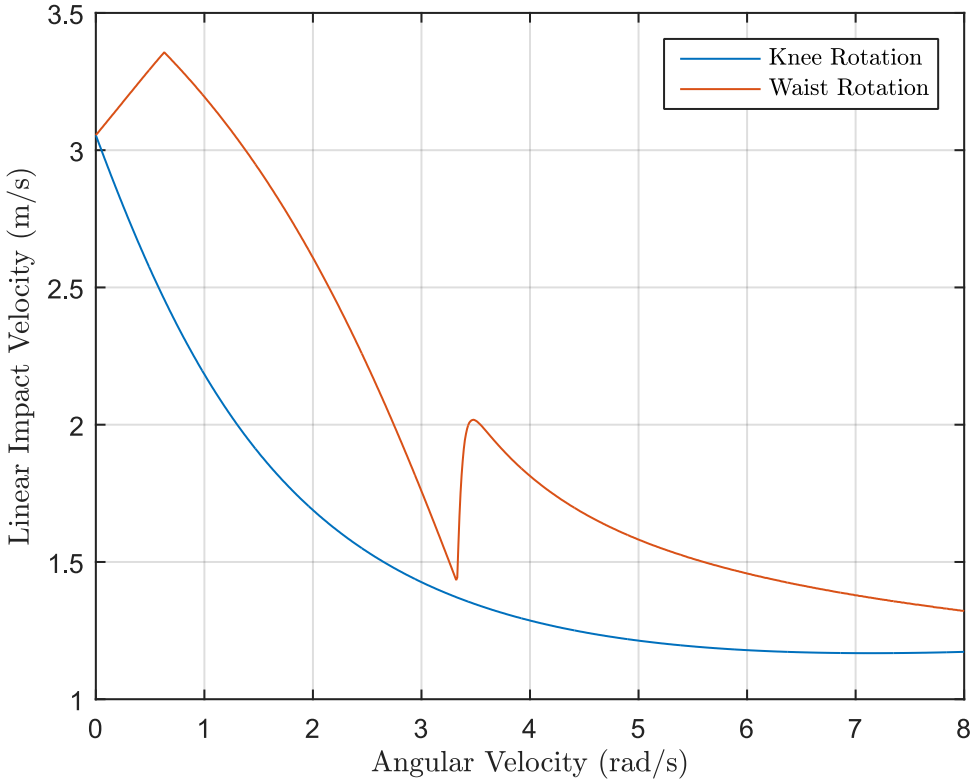

Figure 5.11: Forward Fall COM Impact Velocity vs Joint Angular Velocity

and 3.48 rad/s. The local minimum impact velocity of 1.43 m/s results from the minimum angular velocity required to complete the rotation strategy. After this point the waist hits the joint limit and the body rotates with the effect of gravity and the accumulated angular velocity from rotation of the waist resulting in higher impact velocities. This is due to the now fixed length of the COM pendulum rotating about its pivot rather than decreasing in length as well as rotating. At the higher angular velocities, however, the rotation of the torso hits the joint limit fast enough to not contribute much angular velocity to rotation of the body.

5.4.3 Combined Flexion Results

Combining the two strategies was again done in the same manner as the backward fall. The results of these simulation varying angular velocity of both the knee and waist from 0 to 8 rad/s is shown in figure 5.13. The minimum impact velocity was 0.8 m/s at angular velocities of 4.5 and 7.9 rad/s for the knee and waist respectively resulting in a 72% reduction from the rigid fall impact velocity.

For the minimum impact parameters, rotation of the knee and waist counter each other in terms of whole body rotation. The forward waist rotation, that alone causes an additive effect, in this case is countered by the backward rotation of the knees. This counter rotation causes the COM to reduce significantly without building up much angular rotation during the fall resulting in a significantly reduced impact velocity.

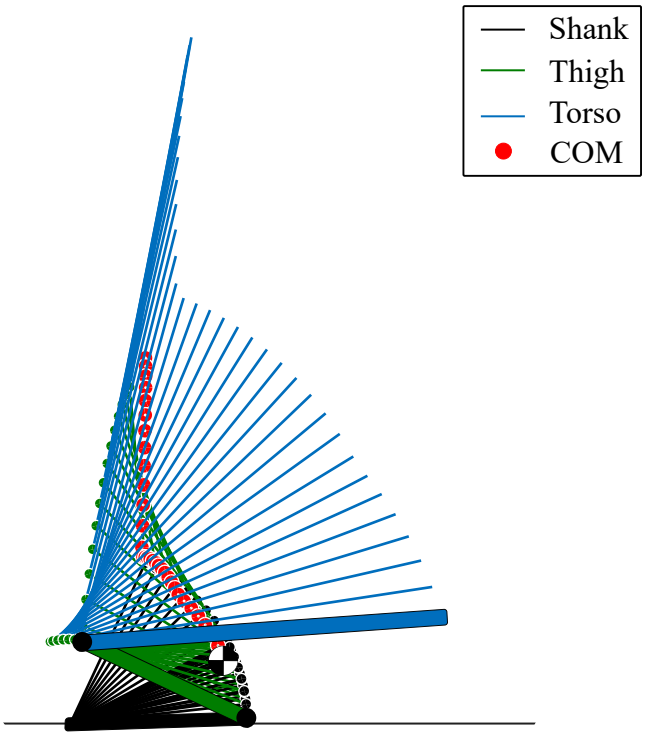

Figure 5.12: Best case forward fall simulation for an initial velocity of 0.25 m/s

It should also be pointed out that the region surrounding a knee rotation of 8 rad/s and waist rotation of 2 rad/s results in rotation of the COM that, according to the work done by Fujiwara et al., would result in a safe knee landing (one where continued rotation after impact at the knees would not occur) [9]. This is why this region has such a low impact velocity as compared to the rest of the possible combinations of parameters.

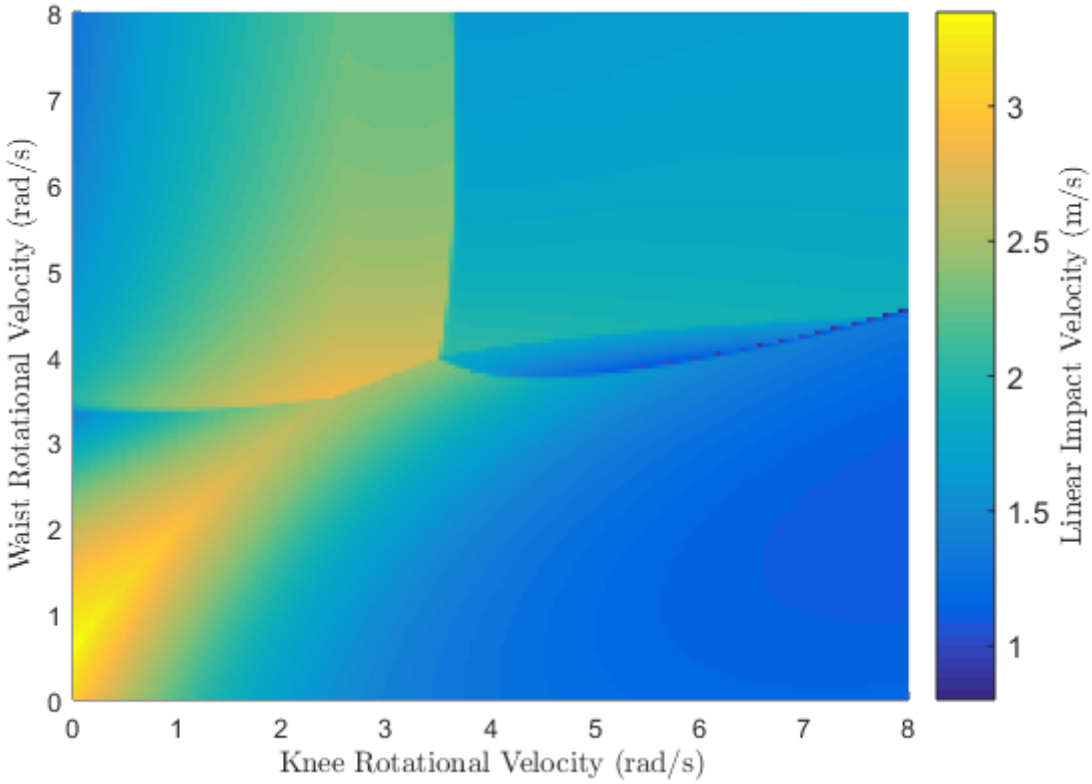

Figure 5.13: Forward Fall COM Impact Velocity vs Simultaneous Joint Angular Velocity

5.5 Combined Flexion Results for Various Initial Conditions

As with the previous two falling cases, since the combined flexion case resulted in the lowest impact velocity of the COM this strategy was used to find the best case parameters for various initial conditions. Similarly the initial linear velocity of the COM was varied from 0 to 1 m/s. These results are shown in table 5.5 below. There is clear trend that constant high knee rotational velocity is required with increasing waist rotation velocity in order to achieve the lowest impact velocity possible. Also, unlike the previous two falling cases the impact velocity increases with initial velocity. This is most likely due to the incredibly short fall time before initial impact with the knees.

Table 5.5: Best Case Backward Combined Falling Strategy Results with Varying Initial Linear Velocity

Initial Vel (m/s)	Knee Vel (rad/s)	Waist Vel (rad/s)	Impact Vel (m/s)
0.0	0.0	0.0	3.49*
0.0	7.30	3.60	0.50
0.1	7.50	3.95	0.60
0.2	7.40	4.20	0.71
0.3	7.60	4.55	0.90
0.4	7.65	4.85	1.06
0.5	7.85	5.20	1.20
0.6	7.70	5.45	1.30
0.7	7.90	5.80	1.45
0.8	7.45	6.00	1.56
0.9	7.80	6.40	1.68
1.0	7.95	6.75	1.79

*Impact velocity for rigid fall shown for reference

5.5.1 Full Degree of Freedom Robot Simulation

Again the efficacy of these strategies was checked using the full degree of freedom robot in Gazebo as shown in figure 5.15. These results are shown in figure 5.14. In this case, waist flexion experienced the highest impact acceleration at 2266 m/s^2 rather than the rigid case at 1733 m/s^2. This is somewhat expected, however, as waist flexion causes the torso to rotate in the same direction as the fall which increases the COM velocity and the local velocity at the tip of the torso which impacts first. Knee flexion and combined flexion however, showed significant decreases in impact velocity with knee flexion resulting in an impact acceleration of 487 m/s^2 and the combined case resulting 239 m/s^2. This resulted in an increase in impact acceleration of 30% for waist flexion and a decrease of 72% and 86% for the knee and combined flexion strategies respectively over the rigid falling case.

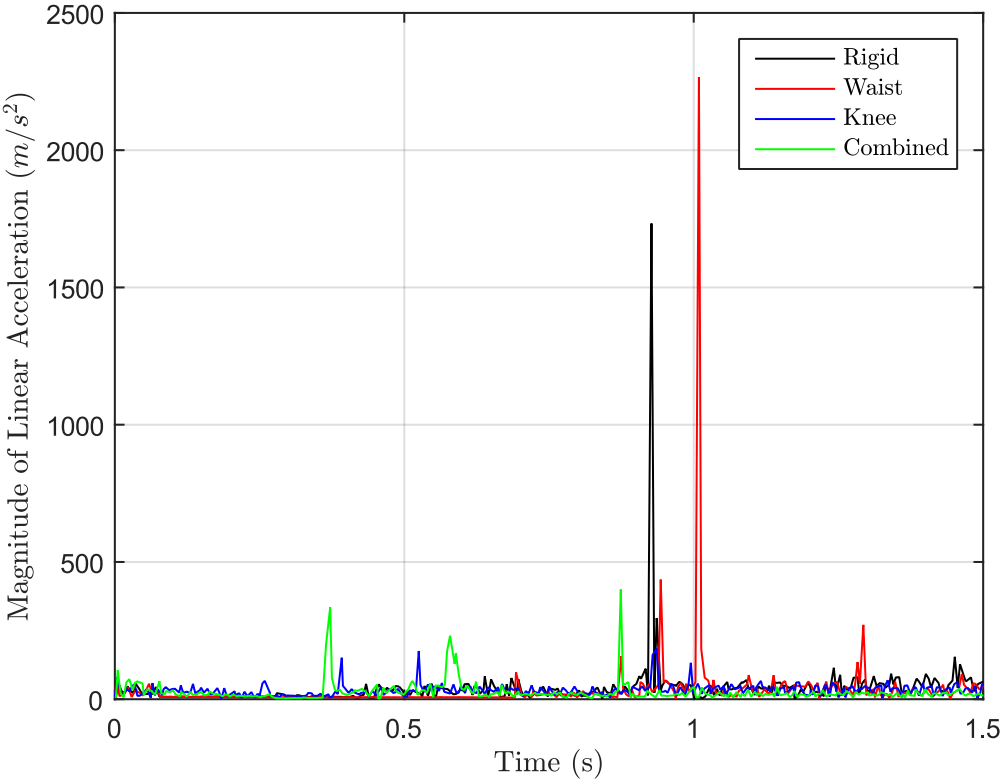

Figure 5.14: ESCHER full degree of freedom forward fall simulation results in ROS Gazebo

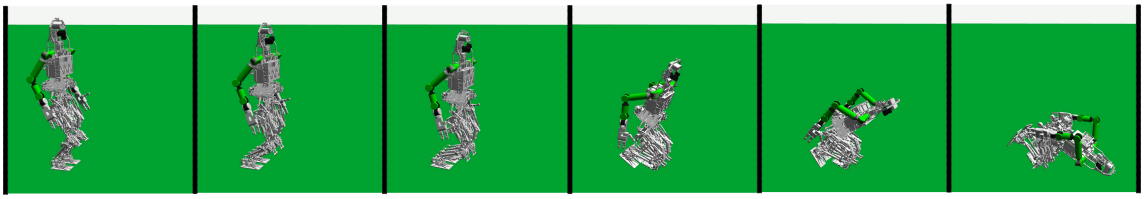

Figure 5.15: ESCHER full degree of freedom forward fall simulation in ROS Gazebo

Chapter 6

Conclusions

In this thesis joint angular velocity falling strategies were studied to reduce the impact velocity of a humanoid robot during a lateral, backward, and forward fall. Each fall case was simulated first with a reduced order model of the robot to test the individual and combined angular velocity strategies and second with a full degree of freedom simulation to prove their efficacy. For each fall case it was determined that a combined joint angular velocity strategy was best to reduce the impact velocity of the robots COM. These reductions using the reduced order models were 58%, 87%, and 74% for a lateral, backward, and forward fall respectively. Various initial conditions were also analyzed and the parameters for minimum impact velocity for each case was determined. This provides a framework for the creation of simple and easy to implement falling strategies that can be used in real time to reduce impact from a standing height fall.

6.1 Future Work

While this work significantly reduces the likelihood of damage to a humanoid robot from a standing fall, it is not necessarily the optimal solution. There may be cases were a fall causes rotation of the body or results in an off axis fall. Also, these analyses did not consider arm motion during the fall. These two areas will be focused on in future work in order to make a more robust and optimal total falling strategy that can be applied in all scenarios to reduce impact as much as possible.

Bibliography

[1] Hopkins, Michael A., Dennis W. Hong, and Alexander Leonessa. "Humanoid locomotion on uneven terrain using the time-varying divergent component of motion." In Humanoid Robots (Humanoids), 2014 14th IEEE-RAS International Conference on, pp. 266-272. IEEE, 2014.

[2] Hopkins, Michael A., Dennis W. Hong, and Alexander Leonessa. "Compliant locomotion using whole-body control and Divergent Component of Motion tracking." In Robotics and Automation (ICRA), 2015 IEEE International Conference on, pp. 5726-5733. IEEE, 2015.

[3] Orlowski, Christopher. "DARPA Robotics Challenge (DRC) (Archived)." Defense Advanced Research Projects Agency. N.p., n.d. Web. 15 July 2017.

[4] Knabe, Coleman, et al. "Designing for compliance: ESCHER, Team VALOR's compliant biped." Journal of Field Robotics (2015).

[5] Knabe, Coleman, et al. "Team VALOR's ESCHER: A Novel Electromechanical Biped for the DARPA Robotics Challenge." Journal of Field Robotics (2017).

[6] Krotkov, Eric, et al. "The DARPA Robotics Challenge Finals: Results and Perspectives." Journal of Field Robotics 34.2 (2017): 229:240.

[7] Fujiwara, Kiyoshi, et al. "UKEMI: Falling motion control to minimize damage to biped humanoid robot." In Intelligent robots and systems, 2002. IEEE/RSJ international conference on, vol. 3, pp. 2521-2526. IEEE, 2002.

[8] Fujiwara, Kiyoshi, et al. "The first human-size humanoid that can fall over safely and stand-up again." In Intelligent Robots and Systems, 2003.(IROS 2003). Proceedings. 2003 IEEE/RSJ International Conference on, vol. 2, pp. 1920-1926. IEEE, 2003.

[9] Fujiwara, Kiyoshi, et al. "Safe knee landing of a human-size humanoid robot while falling forward." In Intelligent Robots and Systems, 2004.(IROS 2004). Proceedings. 2004 IEEE/RSJ International Conference on, vol. 1, pp. 503-508. IEEE, 2004.

[10] Fujiwara, Kiyoshi, et al. "Towards an optimal falling motion for a humanoid robot." In Humanoid Robots, 2006 6th IEEE-RAS International Conference on, pp. 524-529. IEEE, 2006.

[11] Fujiwara, Kiyoshi, et al. "An optimal planning of falling motions of a humanoid robot." In Intelligent Robots and Systems, 2007. IROS 2007. IEEE/RSJ International Conference on, pp. 456-462. IEEE, 2007.

[12] Ogata, Kunihiro, Koji Terada, and Yasuo Kuniyoshi. "Falling motion control for humanoid robots while walking." In Humanoid Robots, 2007 7th IEEE-RAS International Conference on, pp. 306-311. IEEE, 2007.

[13] Ogata, Kunihiro, Koji Terada, and Yasuo Kuniyoshi. "Real-time selection and generation of fall damage reduction actions for humanoid robots." In Humanoid Robots, 2008. Humanoids 2008. 8th IEEE-RAS International Conference on, pp. 233-238. IEEE, 2008.

[14] Cui, Yi Feng, Su Goog Shon, and Hee Jung Byun. "Characteristics of Real-Time Imitation Control for Biped Robot: Falling Time Analysis." In Applied Mechanics and Materials, vol. 427, pp. 983-986. Trans Tech Publications, 2013.

[15] Ma, Gan, et al.. "Bio-inspired falling motion control for a biped humanoid robot." In Humanoid Robots (Humanoids), 2014 14th IEEE-RAS International Conference on, pp. 850-855. IEEE, 2014.

[16] Meng, Libo, et al. "A falling motion control of humanoid robots based on biomechanical evaluation of falling down of humans." In Humanoid Robots (Humanoids), 2015 IEEE-RAS 15th International Conference on, pp. 441-446. IEEE, 2015.

[17] Markoff, John. "Modest Debut of Atlas May Foreshadow Age of 'Robo Sapiens'." NYTimes 11 July 2013

[18] Van den Kroonenberg, A. J., Wilson C. Hayes, and T. A. McMahon. "Dynamic models for sideways falls from standing height." TRANSACTIONS-AMERICAN SOCIETY OF MECHANICAL ENGINEERS JOURNAL OF BIOMECHANICAL ENGINEERING 117 (1995): 309-309.

[19] van den Kroonenberg, Aya J., Wilson C. Hayes, and Thomas A. McMahon. "Hip impact velocities and body configurations for voluntary falls from standing height." Journal of Biomechanics 29, no. 6 (1996): 807-811.

[20] Yun, Seung-kook, Ambarish Goswami, and Yoshiaki Sakagami. "Safe fall: Humanoid robot fall direction change through intelligent stepping and inertia shaping." In Robotics and Automation, 2009. ICRA'09. IEEE International Conference on, pp. 781-787. IEEE, 2009.

[21] Lee, Sung-Hee, and Ambarish Goswami. "Fall on backpack: Damage minimization of humanoid robots by falling on targeted body segments." Journal of Computational and Nonlinear Dynamics 8, no. 2 (2013): 021005.

[22] Goswami, Ambarish, Seung-kook Yun, Umashankar Nagarajan, Sung-Hee Lee, KangKang Yin, and Shivaram Kalyanakrishnan. "Direction-changing fall control of humanoid robots: theory and experiments." Autonomous Robots 36, no. 3 (2014): 199-223.

[23] Kot, Andrzej, and Agata Nawrocka. "Modeling of human balance as an inverted pendulum." In Control Conference (ICCC), 2014 15th International Carpathian, pp. 254-257. IEEE, 2014.

[24] Koenig, Nathan, and Andrew Howard. "Design and use paradigms for gazebo, an open-source multi-robot simulator." In Intelligent Robots and Systems, 2004.(IROS 2004). Proceedings. 2004 IEEE/RSJ International Conference on, vol. 3, pp. 2149-2154. IEEE, 2004.

[25] Spong, Mark W., and Mathukumalli Vidyasagar. Robot dynamics and control. John Wiley Sons, 2008.

[26] Hsiao, Elizabeth T., and Stephen N. Robinovitch. "Common protective movements govern unexpected falls from standing height." Journal of biomechanics 31, no. 1 (1997): 1-9.

[27] Lo, JiaHsuan, and James A. Ashton-Miller. "Effect of upper and lower extremity control strategies on predicted injury risk during simulated forward falls: a study in healthy young adults." Journal of biomechanical engineering 130, no. 4 (2008): 041015.

Appendix A

Center of Mass Full Degree of Freedom Robot

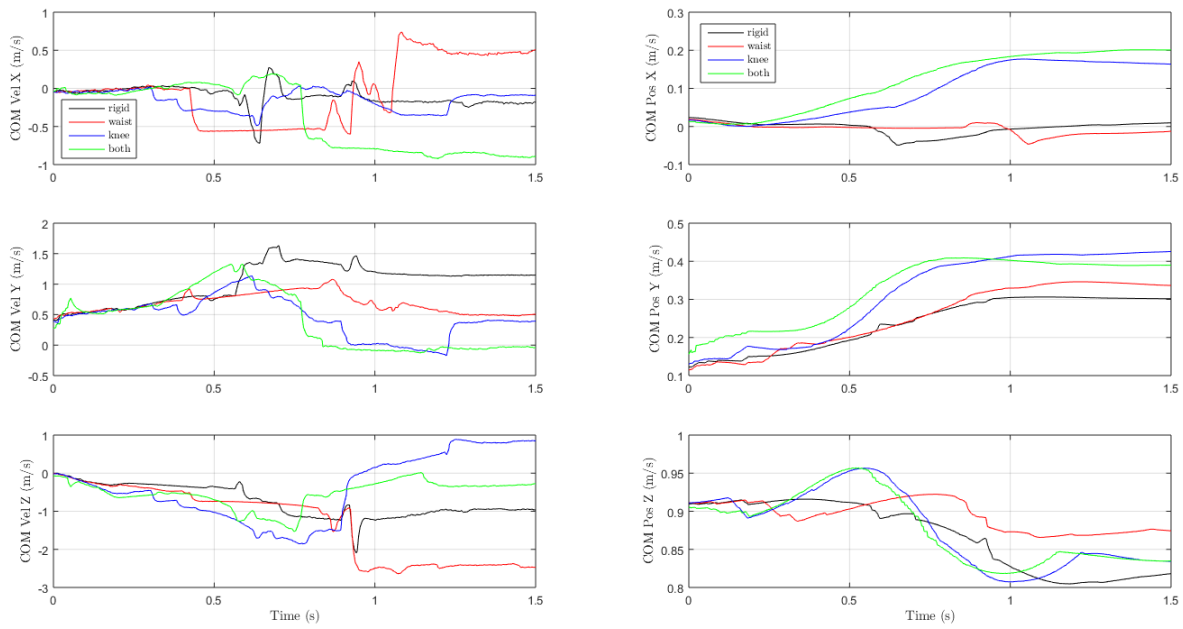

(a) (b)

Figure A.1: Velocities and positions of the COM in X, Y, and Z direction for full degree of freedom falling simulations during a lateral fall. (a) Velocity (b) Position

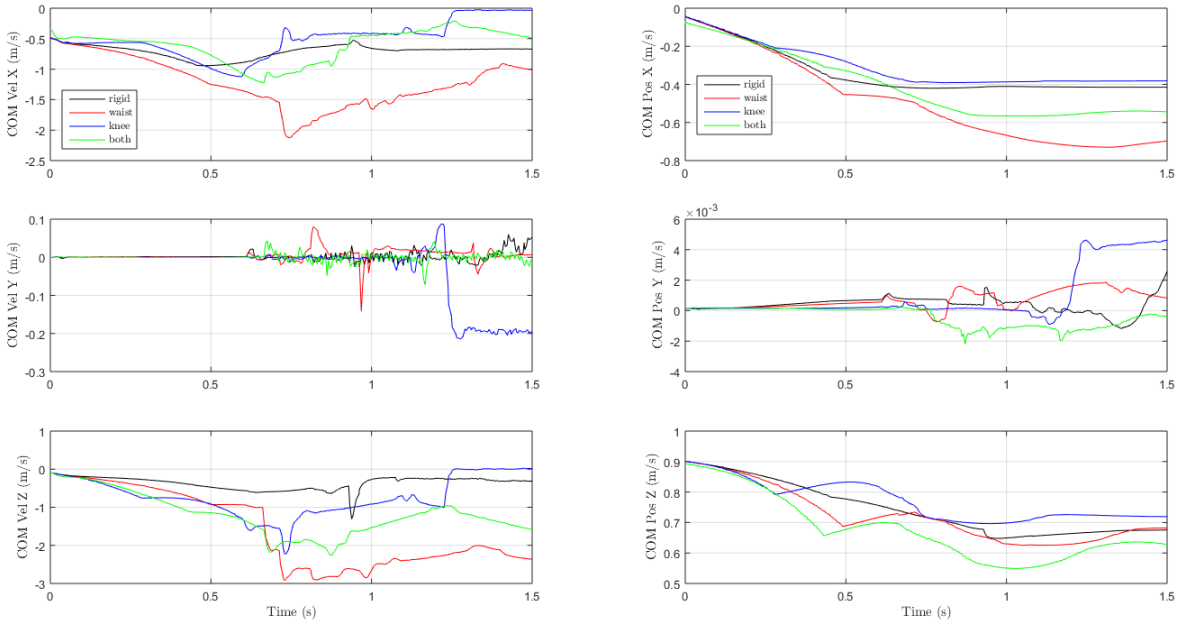

(a) (b)

Figure A.2: Velocities and positions of the COM in X, Y, and Z direction for full degree of freedom falling simulations during a backward fall. (a) Velocity (b) Position

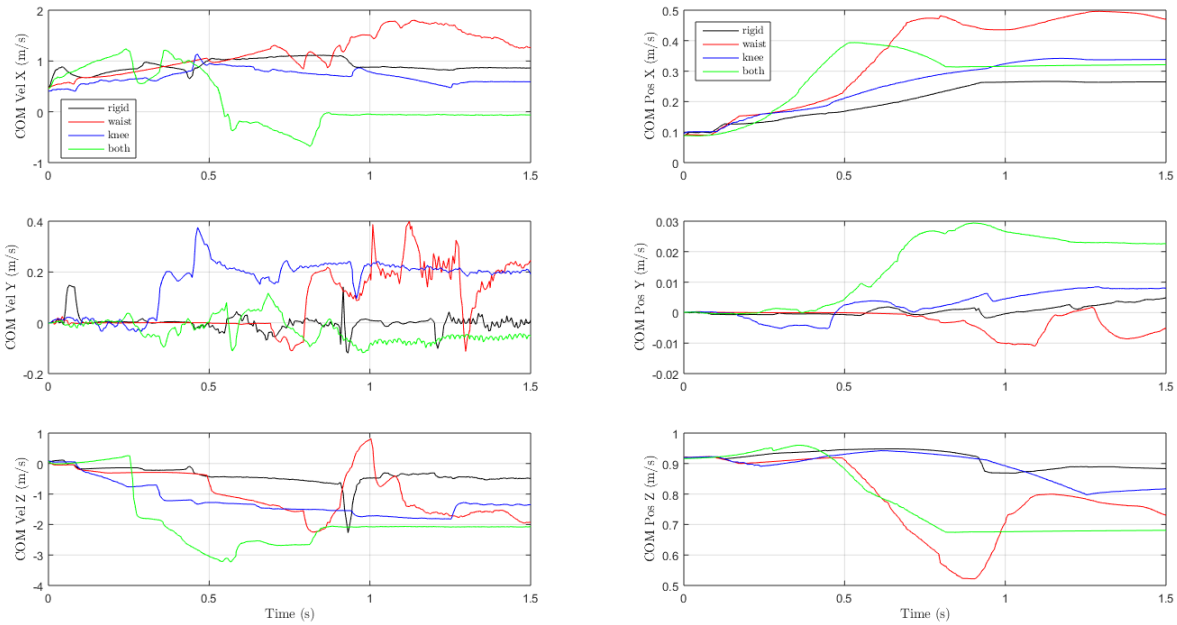

(a) (b)

Figure A.3: Velocities and positions of the COM in X, Y, and Z direction for full degree of freedom falling simulations during a forward fall. (a) Velocity (b) Position